A FUZZY CLASSIFICATION APPROACH FOR MAPPING HETEROGENEOUS AND POORLY SEPARABLE LAND COVER CLASSES

CASE STUDY: THE WEERRIBBEN REEDLANDS IN THE NETHERLANDS

KATUTSI IMMACULATE
February, 2014

SUPERVISORS:
Dr. Ir. W. Bijker
Dr. V.A. Tolpekin

A FUZZY CLASSIFICATION APPROACH FOR MAPPING HETEROGENEOUS AND POORLY SEPARABLE LAND COVER CLASSES

CASE STUDY: THE WEERRIBBEN REEDLANDS IN THE NETHERLANDS

KATUTSI IMMACULATE
Enschede, The Netherlands, [March, 2014]

Thesis submitted to the Faculty of Geo-Information Science and Earth Observation of the University of Twente in partial fulfilment of the requirements for the degree of Master of Science in Geo-information Science and Earth Observation.
Specialization: Geo-informatics

SUPERVISORS:
Dr. Ir. W. Bijker
Dr. V.A. Tolpekin

THESIS ASSESSMENT BOARD:
Prof. Dr. Ir. A. Stein (Chair)
E. Westinga, MSc (External Examiner, University of Twente)

ABSTRACT

This research was done to find a classification method which could be able to map wetland areas defined by reed lands and other land cover classes with heterogeneity and poor separability.
Management of wetlands, which are a crucial eco system and source of economic support, is an important factor in helping to maintain them. Using field surveys is labour intensive and due to nature of wetlands, some areas could be inaccessible. Using remote sensing provides regular and viable information necessary for management of wetlands.

Presence of mixed pixels in remotely sensed images provide a challenge as a pixel cannot be assigned to a single class as provided with conventional classifiers. Soft classification methods can be adopted and in the presence of heterogeneous land cover and lack of clear distinction between classes, fuzzy classifiers may be applied.

This study uses fuzzy classification method based on Maximum likelihood to classify a Geo-eye-1 image of the Weerribben. Probability based classifiers require classes to have normal distribution. The classes in this area possess multimodal distributions which were reduced to sub classes identified from histograms and clustering. Subclasses were analysed using TD and JM class separation measures after which they were either eliminated or allocated to the proper super class. Membership images were produced for individual subclasses using a fuzzy classification. The result is displayed as a series of membership images per class. Accuracy assessment was done for defuzzified result using conventional error matrix and as fuzzy result using FERM.

Pixel based MLC using subclasses resulted in a 14% classification accuracy increase over pixel based MLC using original individual classes. Overall accuracy and kappa coefficient showed poor classification results using fuzzy classification which can be attributed to use of reference data which doesn't correspond to the image classified both in nature (considered crisp in reference data yet fuzzy in nature) and in state (image is acquired at different time than reference data).

This method is able to relatively identify some of the land cover classes (e.g. forest, grassland and reed lands) with moderate accuracy. The ability to define membership of parcels to classes makes this method valuable in providing land cover composition information which can be used in monitoring and maintaining the management types desired for the various plant and animal species in this nature reserve.

Considering the results from this research and the nature of the area, it can be said that with improvement on reference data, fuzzy classification is a good approach for classifying satellite images for mapping heterogeneous and poorly separable land cover. It is possible to some extent to use remote sensing images for mapping reed lands but on their own, they don't provide adequate information for management and have to be used in conjunction with other methods such as field work and aerial photographs.

Keywords:
Remote sensing, mixed pixels, multi modal distribution, intra class variability, Class separability, Maximum likelihood classification, membership function, fuzzy classification, Fuzzy error matrix

ACKNOWLEDGEMENTS

I would like to express my immense gratitude to Dr. Bijker for her invaluable guidance and unwavering encouragement during this research. I also particularly like to thank my second supervisor Dr. Tolpekin for his guidance and advice during this research especially for his enduring patience during programming. I also thank Prof. Stein for his insightful comments which were very instrumental in this work.

I like to thank Chris Tembo, J.C Orena-Billa, Paul Ekallam, and Christine Assimwe who have provided me with great support and advice during the course of my career and education.
I thank my family and friends for their continued support of my endeavours.

Last but not least, I am forever indebted to NUFFIC for this opportunity to further my education, experience cultures from all over the world and meet inspirational people in my career field.

I dedicate this work to my parents J.B.A Katutsi and Provia Katutsi.

TABLE OF CONTENTS

LIST OF FIGURES

LIST OF TABLES

LIST OF ABBREVIATIONS

ASTER	Advanced Spaceborne Thermal Emission and Reflection Radiometer
AVHRR	Advanced Very High Resolution Radiometer
D	Divergence
FERM	Fuzzy Error Matrix
FMLC	Fuzzy maximum Likelihood Classification
FS	Feature Space
IFOV	Instantaneous Field Of View
JM	Jeffries-Matusita
LMM	Linear Mixture Model
MDA	Mixture Discriminant Analysis
MLC	Maximum Likelihood Classification
MODIS	Moderate-resolution Imaging Spectroradiometer
O.A	Overall Accuracy
P.A	Producer's Accuracy
SPOT	Satellite Pour l'Observation de la Terre
SRM	Super Resolution Mapping
TD	Transformed Divergence
U.A	User's accuracy

1. INTRODUCTION

1.1. Motivation and problem statement

Wetlands are an important natural resource and they support a vast eco-dynamic system (Verhoeven et al., 2006). They act as a habitat and provide food for diverse species of animals especially birds, insects and fish. Wetland vegetation including reeds also act as a source of economic product (Schuyt et al., 2004) by providing non-food commodities such as thatch for roofing and paper pulp (Asaeda et al., 2000). Wetlands also act as water purifiers and as flood control by regulating flow of flood water (Hammer et al., 1989).

A dominant reed type found in wetland vegetation is *Phragmites australis,* known as the common reed. Although this plant has been identified as an invading species in some parts of the world (Arzandeh et al., 2003), it has also been recognized as an important part of the wetland ecosystem especially in Europe where it can be directly linked to the survival of specific vulnerable bird species and as support for various recreational and economical activities (Ludwig et al., 2003; Valkama et al., 2008). Extensive monitoring exercises have been carried out to map and monitor reed lands worldwide, most of which involve extensive field studies and remotely sensed images (Asaeda et al., 2000; Pengra et al., 2007)

The Weerribben-Wieden National Park in the Netherlands has the largest un-interrupted peat marsh in Western Europe (Natuurmonumenten, 2011) and reed cultivation is carried out in this area. The government bodies Staatsbosbeheer and Natuurmonumenten which are in charge of maintaining and conserving the area need constant up-to-date information about the land cover to assist in monitoring this area.

Remote sensing methods have been adapted to monitoring the environment including wetlands (Chopra et al., 2001; Jones et al., 2009). Alternative methods to acquire information for monitoring such as the use of aerial photography and land based surveys are labour intensive, take a long time and are expensive as well. Use of satellite imagery for land cover and land change studies is greatly influenced by their classification accuracy. 'In practice, the choice of classification methods has to be suited to the nature of land cover in question as this can strongly affect the result of the classification' (Burrough et al., 1998).

Some of the land cover classes in the Weerribben are defined as the following; grasslands rich in herb and fauna, croplands rich in herb and fauna, grasslands for recreation, vegetation with shrubs and herbs, dry nutrient-poor soil with rare plant species, and wet nutrient-poor soil with rare plant species, among others. Due to the heterogeneous nature of this land cover which is characterized by mixtures of plant species and fuzzy boundaries between water and vegetation classes, there is intra and inter class variability, making the use of traditional hard classification methods inadequate. More so, the parcels in this area are small in size which leads to mixed boundary pixels in images which do not have very high spatial resolution.

Soft classification methods such as fuzzy classification, linear mixture modelling (LMM) and mixture discriminant analysis (MDA) have been employed to map vegetation types (Ju et al., 2003; McMahan et al., 2003; Quintano et al., 2013; Xie et al., 2008). Due to the heterogeneity of vegetation cover in this area, fuzzy classification methods may be implemented in classifying this area. In fuzzy classification, a pixel is assigned various classes whose contribution to the pixel is determined by a membership value.

Due to the nature of and size of parcels, obtaining training data for the many classes in such an area can be difficult. And also the narrow parcels make is easy to include boundary pixels in training samples. Therefore, the availability of a management map which provides demarcation of parcel boundaries minimizes the possibility of inaccuracies in training data by restricting training samples to pixels fully contained within the required parcels.

1.2. Research idenfication

Staatsbosbeheer and Natuurmonumenten have defined, in their management map, land cover classes for the area. These classes are, for the most part, usually a mixture of similar plant species but in different proportions. The most widespread plant is reeds which aside from growing on reedlands, can be found on quaking bog, swamp and forest parcels and also on the ridges, identified as moist soil and wet soil, which separate the reedland parcels. Because the classes defined in the study area have similar composition of land cover, their end members can be expected to be spectrally very close and therefore classification of the image will be poor if hard classification methods are used. A classification approach that can handle heterogeneity in land cover classes which have poorly separable spectral signatures is therefore required.

Vector boundary information is incorporated to obtain pure class samples in training data. Due to the mixed nature of the land cover classes in this area, it is required that individual classes be considered super classes which are made up of subclasses.

1.2.1. Research objectives

The main objective of this research is to define a method for classification of areas with land cover classes which are poorly separable and have high intra class variability.

The sub- objectives are as follows;

- To define the super classes and the nature of distribution of their associated spectral data.
- To investigate and implement an appropriate classification algorithm which can distinguish heterogeneous and poorly separable land cover classes with fuzzy boundaries.
- To obtain accuracy assessment of the classification-result and review its application in management of the area.

1.2.2. Research questions

The following questions will be answered to obtain the above mentioned objectives.

- What are the major land cover classes in this area and what is the relationship between management classes defined in the management map and land cover from visual interpretation of the image?
- What is the nature of the distribution of spectral data associated with the identified land cover classes?
- What are the criteria for defining the subclasses?

- How can the relationship between super classes and corresponding subclasses be interpreted?
- What classification method is appropriate to classify the image as defined by its super and sub classes, and in distinguishing poorly separable classes?
- What accuracy assessment procedure best describes the result of the classification used?
- How can the classification result be used in making management decisions for this area?

2. LITERATURE REVIEW

This chapter introduces the theories which support and provide insight into the procedures adopted during this research.

2.1. Background

2.1.1. Remote sensing and wetland mapping

Wetlands are defined as the areas of transition between water bodies and ground. They are characterised by various types of plants, shallow pools of water and animals especially birds. Wetlands form an important ecosystem which serves economic, environmental and social purposes (Hammer et al., 1989; Schuyt et al., 2004).

Management and monitoring of wetlands requires information which is a result of consistent and accurate interpretation of the wetland land cover properties. The need to preserve and maintain wetlands is high. Various means have been applied to this end, some of which include field surveys, aerial photographs, collateral ancillary data and remote sensing imagery (Arzandeh et al., 2003; Asaeda et al., 2000; Lyon et al., 1992). Data collection is traditionally done through field surveys and aerial photographs. Remote sensing methods provide regular and valuable information that may not be readily supplied by other means. And also due to the nature of most wetlands, some of these areas are inaccessible leaving remote sensing as the only viable alternative.

With a wide range of sensors used in remote sensing of vegetation including wetlands, classification approaches have been developed which suit each individual sensor. The different spectral, spatial and radiometric resolutions of different sensors make them suiTable for monitoring specific land cover types. Vegetation has been widely monitored using MODIS and AVHRR at global scale, LandSAT, SPOT, ASTER at regional scale and IKONOS, Quickbird, Aviris and Hyperion imagery at a local scale (Nagendra et al., 2008; Xie et al., 2008).

2.1.2. Mixed pixels in remote sensing

Wherever satellite imagery is concerned there will always be a question of mixed pixels more often because the pixel captures more area on the ground than a user would like and also depending on the nature of element being sensed (Cracknell, 1998).

Mixed pixels occur when the instantaneous field of view (IFOV) of a sensor captures more than one element on the ground and/or when the phenomenon being captured has heterogeneity in nature that is captured within the dimensions of a pixel (Foody, 2004). There are four documented types of mixed pixels ; sub pixel, boundary pixel, inter grade and linear sub-pixel (Fisher, 1997) as shown in Figure 2-a.

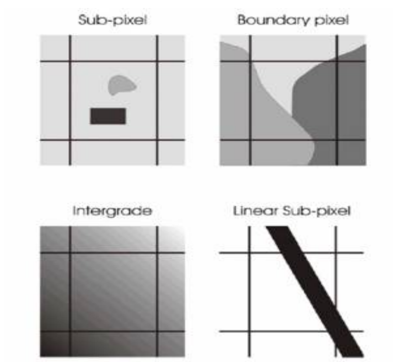

Figure 2-a: Types of mixed pixels encountered in satellite images (Fisher, 1997). They represent cases of objects which are (1) smaller than pixel size, (2) have boundaries crossing over pixel, (3) gradually change in content and (4) linear in nature causing them to be contained in many pixels.

Mixed pixels present a problem in image classification because traditional hard classification methods assume that each pixel represents one class(Thomas et al., 1987) . In practice however, it is common that a pixel will contain elements belonging to more than one class(Atkinson, 2005).

2.1.3. Remote sensing image classification methods

Supervised methods and unsupervised methods including hybrid classification methods have been formulated over time to obtain accurate classification of wetland areas. These can be grouped into hard classification methods and soft classification methods (Xie et al., 2008).

Presence of mixed pixels leads to preference of soft classifiers which include sub pixel classifiers and fuzzy classifiers. Sub pixel classifiers define fractions of classes within a pixel and are more suited to mixed pixels whereas Fuzzy classifiers are suited to classification of vague classes (Xie et al., 2008). In fuzzy classification, a pixel is assigned various classes whose contribution to the pixel is determined by a membership value (Zhang et al., 1998). Sub pixel classifiers include and are not limited to linear mixture models, artificial neural networks, classification trees and hybrid maximum likelihood classification methods among others (Xie et al., 2008).

Sub pixel classification methods such as Super resolution mapping (SRM), Linear Mixture Modelling (LMM) and Mixture Discriminant Analysis (MDA) have been employed to map vegetation types (Ardila et al., 2011; Ju et al., 2003; McMahan et al., 2003; Quintano et al., 2013; Xie et al., 2008). Due to the heterogeneity of vegetation cover in wetland areas, it may be useful to implement fuzzy classification methods in classifying them.

2.2. Fuzzy sets and fuzzy classification

In instances where the land cover has fuzzy properties e.g. in boundary or in composition, fuzzy classification methods can be adopted. These are derived from fuzzy set theory and they assign a pixel to multiple classes with varying strength termed as class membership.

Fuzzy classification is based on fuzzy set theory. Whereas conventional or crisp sets allow only binary memberships, fuzzy sets consider the possibility of partial membership. Fuzzy sets are adaptations of crisp sets which accommodate situations where class boundaries cannot be sharply defined (Richards, 2013).

Crisp sets and fuzzy set scenarios are shown in equation (2.1) and (2.2) respectively;

$$X_A: X \to \{0,1\} \quad \text{where } x_A(X) = \begin{cases} 1 & if\ X \in A \\ 0 & if\ X \notin A \end{cases} \tag{2.1}$$

Equation (2.1) defines a crisp set whose values are 1 if an element is a member of a class and 0 otherwise.

$$\mu_A : X \to [0,1] \quad \text{Where } \mu_A(X) \text{ is the membership value of } X \text{ in } A. \tag{2.2}$$

Different cases of fuzzy set models are shown in Figure 2-b.

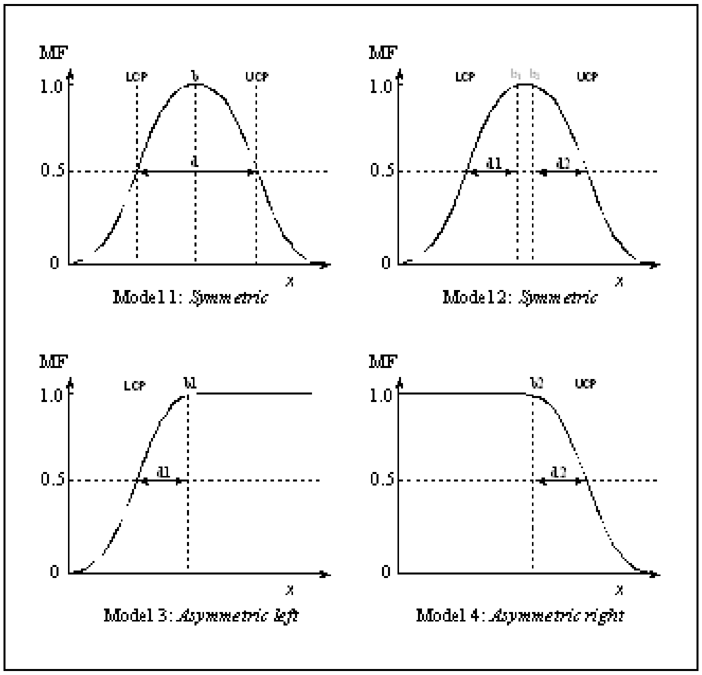

Figure 2-b:Fuzzy set models (Burrough et al., 1998). MF denotes Membership value, d1 and d2 are width of transition zones, LCP and UCP are upper and lower crossover points and b1 and b2 are values at the ideal point.

Fuzzy sets are adaptations of crisp sets to accommodate situations where class boundaries cannot be sharply defined. Membership functions are generated to define the region of transition. With fuzzy membership, a pixel is considered to belong to more than one class by a weighted measure known as membership. This is usually normalised such that for a given pixel,the sum of memberships to classes will be equal to 1. Memberships range from 0 to 1 with 1 indicating maximum.

The membership value corresponds to the strength with which the class is represented in the pixel. Fuzzy memberships can be derived from various classification methods both unsupervised and supervised. These include among other fuzzy c-means, neural networks and fuzzy maximum likelihood classification (FMLC). The output of fuzzy classification is displayed as a series of membership images showing the grade of membership of a class in all pixels in the image.

2.2.1. Maximum likelihood classification and Fuzzy membership based on Maximum likelihood classification

Maximum likelihood classification (MLC) is a method commonly used in classification of satellite images and is the basis for most probability classifiers that have been developed.

MLC depends on having a data distribution approximated by normal Gaussian 'multivariate normal distributions' for each class. If this isn't the case, for example with multi modal classes, the accuracy will suffer. It's important to evaluate data distribution before applying MLC. Multimodal classes should be resolved into subclasses at the training stage , to decrease classification error (Richards, 2013).

The probability of a pixel belonging to a certain class is modelled after a likelihood and prior probability, an implementation of Bayes' criteria.
A major assumption made with maximum likelihood is that the classes are normally distributed, as described above. Considering the class statistics, i.e. mean and covariance, each pixel in the image is assigned to a class to which it has the highest probability.

The probability of a pixel y to belong to a class ω is given by;

$$P(y|\omega = k) = \frac{1}{(2\pi)^{\frac{n}{2}}} \frac{1}{\sqrt{|C_k|}} \exp\left(-\frac{1}{2}(y - \mu_k)^{\mathrm{T}} C_k^{-1} (y - \mu_k)\right) \quad (2.3)$$

Where;
k = index of class
$y = n$ dimensional data (where n is the number of bands)
$p(w_k)$ = probability that class ω_k occurs in the image
$|C_k|$ = determinant of the covariance matrix of the data in class ω_k
μ_k = mean vector
T = transpose function.

Pixel y is assigned a class ω where k has the highest probability.

Fuzzy Maximum likelihood Classification is based on both probability theory and fuzzy set theory. Here probabilities are estimates of the likelihood of full membership in each class. In conventional MLC, the highest probability is used to assign a pixel to a class, with fuzzy MLC; probabilities of all candidate classes for a pixel are reported. These values are then normalised so that they have lower and upper bound of 0 and 1 after which they are referred to as membership values and they are a measure of the possibility of a pixel belonging to a candidate class. This procedure however pragmatic/intuitive has no theoretical proof as yet. Burrough et al. (1998)

2.2.2. Accuracy assessment of FMLC

Accuracy assessment helps in defining suitability for intended use of the result of classification and guides the decisions that can be made with that result (Congalton et al., 2008; Richards, 2013). From results of accuracy assessment, the mapping exercise can be examined for errors in reference data, sensitivity of the classification to observer variability, inappropriateness of remote sensing technology used for mapping that land cover and also mapping errors. Knowledge of this assists in directing the use of the map to where it is most applicable (Richards, 2013).
The accuracy of a fuzzy classification can be assessed by assigning a pixel to the class to which it has the highest membership (Bardossy et al., 2002) and using conventional methods of computing confusion matrix and kappa co-efficient as required (Zhang et al., 1998). However this is process, leading to defuzzification of the data, loses the property of fuzziness and the improvement which it adds and therefore evaluating the accuracy of a fuzzy classification using conventional accuracy assessment methods will result in inaccurate assessment as these are only suited to hard classification (Foody, 1996).

The error matrix has been widely accepted as a standard measure for the accuracy of thematic maps. For fuzzy classifiers, this has to be adjusted so that it takes into account fuzziness in both ground data and/or classified data. Binaghi et al. (1999) discussed and implemented a method known as a fuzzy error matrix (FERM) which combines the properties of an error matrix with some measure of fuzziness. The FERM allows for fuzziness in both ground control data and in the classified data. It can be implemented in cases where fuzziness is apparent in the ground control data and/or the classified data. FERM provides more accurate description of a fuzzy classification result as opposed to the traditional error matrix (Congalton et al., 2008).

With FERM, the Min fuzzy operator, decides the intersecting membership value which is assigned to the classes in the considered pair of classes (Binaghi et al., 1999). The results returned in this FERM are user producer and overall fuzzy accuracies as defined by the row, column and diagonal values respectively. An improvement on the accuracy assessment is the use of kappa statistic which takes into consideration and minimises the possibility of chance agreement in the calculated accuracies. The resulting kappa value is one free of chance agreement.

2.3. Training strategy/procedure

Classification of remotely sensed images involves two major procedures, (1) identifying training pixels and finding their associated statistics (training) and (2) assigning the pixels within the image to a particular class using the defined class statistics (classification).

There has been a lot of research concentrated on modifying classification algorithms to obtain better classification results. These include and aren't limited to fuzzy classifications, neural networks, image segmentation and methods incorporating spatial contextual information among others.

However, it was also identified that the form of training procedure used also affected accuracy of final results. This is because an important assumption made is that training data is representative of the spectral signatures of each class and therefore, apart from the algorithm used, the type of training data can influence the accuracy of the overall classification result (Campbell, 1981; Hixson et al., 1980). There is however no single best way to carry out training as this is dependent on the application, classifier, study area, budget and limitations among others (Richards, 2013).

It has been established that for probability based (parametric) classifiers like maximum likelihood, training data should contain pure pixels and the number of pixels per class should be greater than the number of dimensions of the data. Also, a study by Chen et al. (2002) found that 'for spatially heterogeneous classes, small block training has the advantage of readily capturing spectral and spatial information.' This is where training samples are selected as multiple blocks (a group of pixels) over the site.

2.4. Class separability

Class separability is a statistical quantitative measure of how well classes can be separated. They are computed from class statistics i.e. mean, standard deviation and covariance.

The simplest class separability measure is the Euclidian distance which is the distance measured between the means of two classes. This measure doesn't take into account variability and correlation existing between classes. More accurate measures which account for higher order statistics such as covariance have been defined. These include among others Divergence, Transformed Divergence (TD), Jeffries-Matusita (JM), Battacharya, Mahalanobis distance measures (Schowengerdt, 2006).

Divergence takes into account the within-class variation in addition to class means and it ranges from 0 to infinity. It has the disadvantage that it tends to show increasing separability when that is not the case and at large separations, small increments will lead to much better accuracy in classification, due to its nature of quadratic increase with separation, which isn't the case in practice (Richards, 2013). This drawback doesn't affect JM measure.
Divergence D is computed as;

$$\mathrm{D} = \frac{1}{2}\mathrm{tr}\left((C_i - C_j)(C_i^{-1} - C_j^{-1})\right) + \frac{1}{2}\mathrm{tr}\left((C_i^{-1} - C_j^{-1})(\mu_i - \mu_j)(\mu_i - \mu_j)^{\mathrm{T}}\right) \qquad (2.4)$$

Where;
i and j = the two classes being compared
tr = the trace function (matrix algebra)

Unlike divergence, Transformed Divergence and Jeffries-Matusita have lower and upper bounds and are therefore preferred in comparing class separability.

2.4.1. Jeffries-Matusita (JM)

The formulas for Bhattacharya distance and Jeffries-Matusita are as follows;

$$B_{ij} = \frac{1}{8}(\mu_i - \mu_j)^T \left(\frac{C_i + C_j}{2}\right)^{-1} (\mu_i - \mu_j) + \frac{1}{2}\ln\left(\frac{|(C_i + C_j)|/2}{\sqrt{|C_i||C_j|}}\right) \qquad (2.5)$$

$$\mathrm{JM_{ij}} = 2\left(1 - \mathrm{e}^{-B_{ij}}\right) \qquad (2.6)$$

Where B_{ij} is Bhattacharya distance
JM provides a measure of the distance between two classes in a given set of bands and has a lower bound of zero for identical classes and an upper bound of 2 for perfectly separated classes.

2.4.2. Transformed Divergence (TD)

The formula for Transformed Divergence is as follows;

$$\mathrm{TD_{ij}} = 2\left(1 - \exp\left(\frac{-\mathrm{D_{ij}}}{8}\right)\right) \qquad (2.5)$$

Where $\mathrm{D_{ij}}$ is Divergence.
The formula for Transformed Divergence is reached empirically without any theoretical foundation. The scale of the divergence ranges from 0 to 2. As can be seen from its equation, there's an exponential decrease in the weight applied to increasing distances between classes. It is therefore able to provide realistic values even at great separations between classes, something which isn't possible with the Euclidian distance measure. The upper bound is approached asymptotically.

JM is less computationally efficient than TD when dealing with images which have a high number of spectral classes. With TD and JM values ranging from 1.9 – 2, 1.7-1.9 and 0-1.7 indicate clear, moderate and poor separability between classes, respectively. (Richards, 2013).

2.5. Intra class variability and multimodal data distribution

Heterogeneous land cover types characterised by vegetation may have both inter class variability and intra class variability. The latter is caused by elements in individual classes having different spectral signatures. Intra class variability can be identified by examining the distributions of such heterogeneous classes and they will show multi modality in form of multi modal histograms (Figure 2-c) and multiple clusters in the feature space.

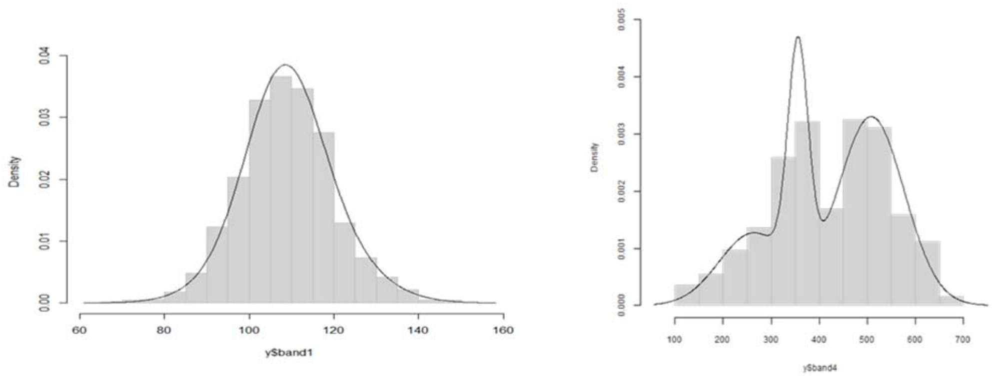

Figure 2-c: Unimodal and multi- modal distribution shown by histograms fitted with density curves (solid line). Band 4 data values (x axis) are plotted against density (y axis). The number of peaks (modes) defines the presence of different singular distributions. More than one mode shows multimodality as shown in the right plot.

Intra class variability can be due to biophysical and biochemical properties of the vegetation cover for example chlorophyll content, age, amount of leaves and bark etc (Song, 2005). Intra class variability poses a problem in image classification. Classification methods such as MLC require that multi-modality in classes be corrected for prior to classification by defining classes into unimodal subclasses (Richards, 2013). A study by Foody et al. (2006) showed that intra class variability has a negative impact on the accuracy of a soft classification. Therefore it needs to be accounted for to obtain higher accuracy.

3. STUDY SITE AND DATA

This chapter introduces the study area, its nature and the activities that define its present landscape, and the data, multi spectral image and management map, which is used in this research.

3.1. Study site

The Weerribben Wieden national park is located at 52° 38'- 52° 48' North, 5° 53' - 6° 08'East, north west in the province of Overrijssel in the Netherlands. It covers an approximate area of 10,000 hectares.

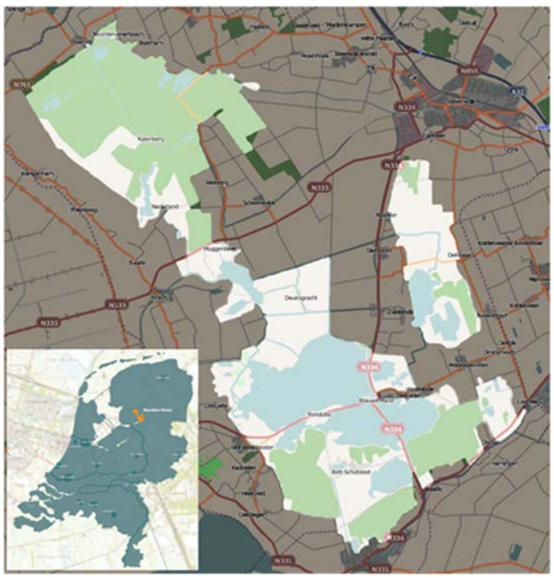

Figure 3-a: The Weerribben-Wieden National Park (Wikipedia, 2014) and The Wieden (Natuurmonumenten, 2011) L-R. They are nature reserves which form some of the important wetlands in Europe. Extensive flooding in The Wieden arose due to poor peat mining methods.

3.1.1. Practices

The Weerribben and Wieden form a cultural landscape with the unique nature of the area being a result of human intervention in the area. Extensive peat mining was the major activity and this led to a rectangular landscape of ditches and ridges (as seen in Figure 3-c). Peat was excavated from the ditches also known as peat holes and dried and transported along the ridges. In the earlier years, due to excessive excavation of peat in the lower part of this area (the Wieden), the ridges collapsed leading to irreversible extensive flooding as shown in Figure 3-a.

This prompted cautious measures to be taken with the remaining areas to avoid like circumstances and in the early 19th Century peat mining was abandoned and reed farming became the dominant activity in this region. The area was later designated as a protected nature reserve due to the realization of its potential as an important ecosystem and has the largest un-interrupted peat marsh in Western Europe. Along with reed cultivation, the area reclaimed from reed growing has evolved to become a habitat for various rare plant and animal species.

3.2. Data

3.2.1. Multispectral image

The area was captured in a Geo-eye-1 image taken on 24th October 2011. It has a projection of UTM Zone 31 and four bands, 1-4, corresponding to Blue, Green, Red and Near infrared respectively.

Table 3-a: Spectral properties of Geo-eye1 image

Band	*Description*	*Spectral range (µm)*	*Spatial resolution(m)*
Band 1	Blue	0.45 to 0.51	1.65
Band 2	Green	0.51 to 0.58	1.65
Band 3	Red	0.655 to 0.69	1.65
Band 4	Near Infra Red	0.78 to 0.92	1.65
Band PAN	Other	0.45 to 0.8	0.41

Figure 3-b: Geo-eye-1 image of The Weeribbeen (true colour image) and photo of partially mowed reed field. Reed farming is extensively carried out in this area with mowing taking place in summer and winter seasons.

3.2.2. Image subsets

Various subsets were taken over the image which was used in this study. A large subset was required for obtaining training data. Subsequent smaller subsets were used to test the results for validation. The subsets are shown in the Figure 3-d.

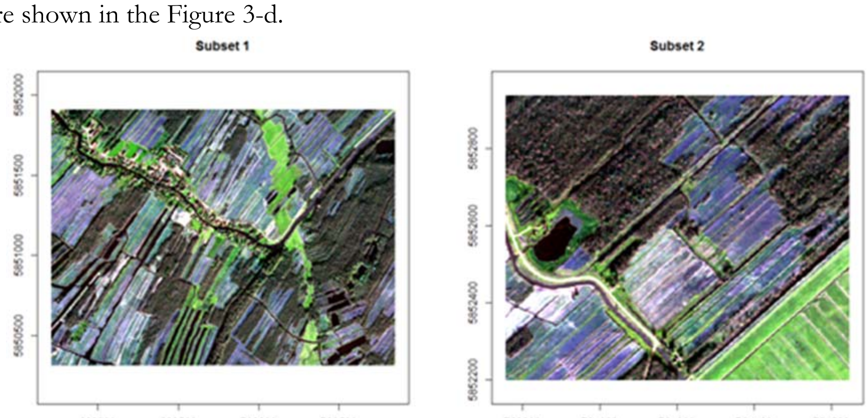

Figure 3-c: True colour combination images (3, 2, 1 in RGB) of subsets taken from the study area for analysis. Subset 1 was used to extract training data and subset 2 is used in verification.

'Subset 1' was selected in such a way that it contained a reasonable number of parcels in all classes that were required for analysis. It covers an area of 798x1070 pixels. 'Subset 2' which was used for verification covers an area of 335x445 pixels.

3.2.3. Management map

The management map provided for the Weerribben was obtained by manual digitising based on aerial photographs of the area which were captured on December 29, 2008 and had spatial resolution of 25 cm. It was updated with data from field work carried out up to December 2012. Several issues were taken into consideration or observed during this process some of which are as follows;

- Some of the parcels were irrigated and appeared flooded and so were digitized as water.
- Cropland and crops aren't digitized.
- Winter mowed parcels are registered, however not all summer mowed parcels are registered.
- The management type of forest included shrubs.
- Forest (tree canopy) sometimes overlaps water and along forest and water ways some parcels aren't filled in and so there are gaps in the map.
- Some features were too small and were omitted because of the difficulty which they would introduce without adding value to the map (for example small pockets of water).

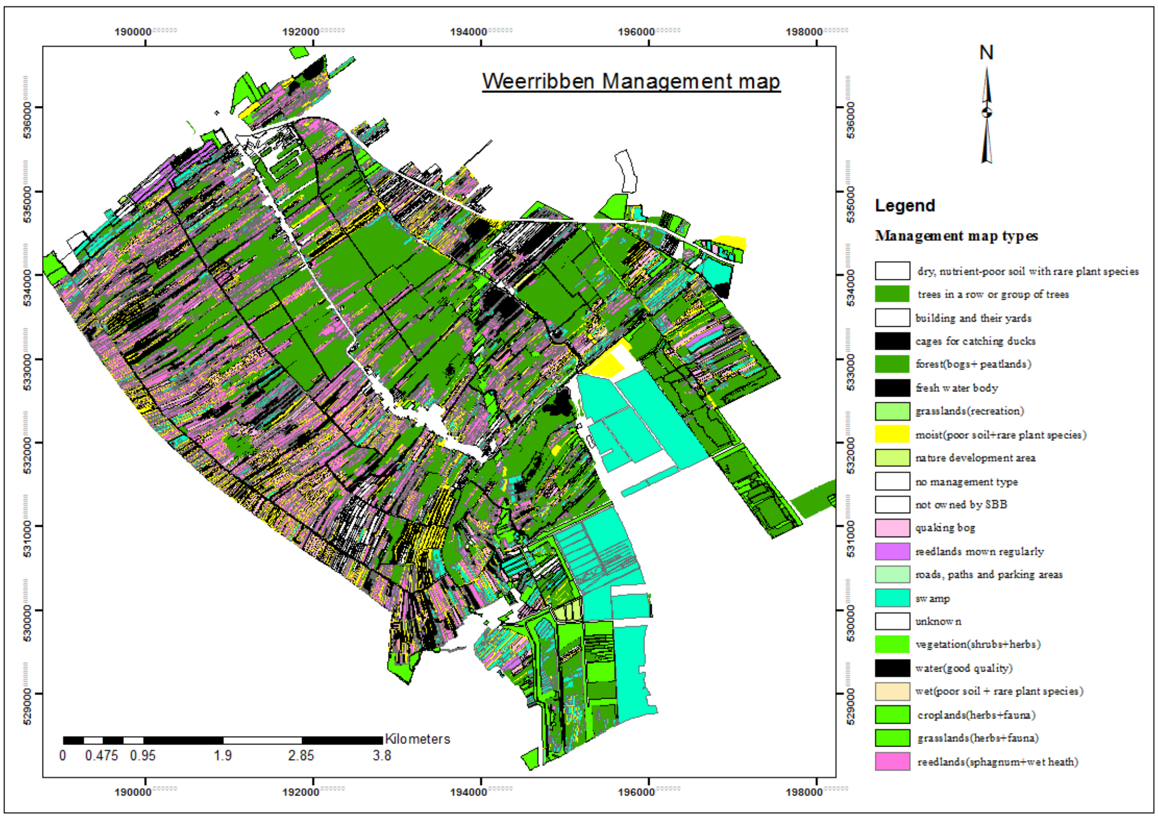

Figure 3-d: Thematic map of the management types in the Weerribben. Most parcels are rectangular and are separated by narrow ridges of wet, moist or poor soil. Management of this area involves practices such as mowing and irrigation.

Table 3-b: Parcel labels as provided in the management map. Some of the parcels have no attached management type, are labelled unknown and are not owned by SBB. These have no land cover information attached to them.

Class code	SBB Identified as	Description
1	*Bossingel en bosje*	Trees in a row or group of trees
2	*Droog schraalland*	species
3	*Eendenkooi*	Cages for catching ducks
4	*beheer*	Building and their yards
5	*Geen beheertype*	No management type
6	*Geen eigendom sbb*	Not owned by SBB
7	*Gemaaid rietland*	Reed lands mown regularly
8	*Hoog- en laagveenbos*	Forest(bogs and peat lands)
9	*Kranswierwater*	Water(good quality)
10	*Kruiden- en faunarijk grasland*	Grasslands(herbs and fauna)
11	*Kruiden- en faunarijke akker*	Croplands(herbs and fauna)
12	*Moeras*	Swamp
13	*Nat schraalland*	Wet(poor soil and rare plant species)
14	*Nog om te vormen naar natuur*	Nature development area
15	*Onbekend*	Unknown
16	*Recreatieweiden*	Grasslands(recreation)
17	*Ruigteveld*	Vegetation(shrubs and herbs)
18	*Trilveen*	Quaking bog
19	*Veenmosrietland en moerasheide*	Reed lands(sphagnum and wet heath)
20	*Vochtig schraalland*	Moist(poor soil and rare plant species)
21	*Wegen, paden en parkeerterreinen*	Roads, paths and parking areas
22	*Zoete plas*	Fresh water body

The provided management types were grouped into land cover classes. Those types which have similar land cover type were combined into one land cover class as shown in Table 3-c. Built up areas, roads and parcels which were undefined and which aren't important in this study were grouped into a single class with label 'unclassified'.

Table 3-c: Class allocation of management classes to land cover classes. Management types which had similar land cover properties were combined into one class. Undefined parcels with no management type and those containing roads and building were combined into the Unclassified class.

Class ID	Class code	Class
1	7,19	Reedlands
2	8	Forest
3	10,16	Grasslands
4	12	Swamp
5	13	Wet
6	18	Quaking bog
7	20	Moist
8	3,9,22	Water
9	1,2,4,5,6,11,14,15,17,21	Unclassified

3.3. Software used

Erdas 2013.2 and ArcGis 10.2: These were used for geo-referencing vector file and editing management map.

Envi 5.0.2: This was used in image analysis and analysing the class signatures

R 0.97.551: Package rgdal, raster, and rgl packages were used to formulate algorithm for training, clustering generating class statistics and in image classification.

4. METHODOLOGY

4.1. Data preparation and pre-processing

This section introduces the procedures carried out on the data as it was provided to make it suiTable for analysis required in this research.

4.1.1. Image pre-processing

Histogram stretching was applied to the image. This adjusted the minimum and maximum DN values of the pixels to a range of 0 to 255.

$$g(x,y) = \left(\frac{f(x,y) - 0}{225 - 0}\right)255 \tag{4.1}$$

Where $f(x,y)$ and $g(x,y)$ are the original and final intensity values of each pixel value after stretching.

4.1.2. Vector file pre-processing

The vector file, which was referenced to the Dutch reference system, was re-projected to the coordinate system of the Geo-eye-1 image, which was on UTM Zone 31, WGS 84.
On critical inspection of the resulting overlay of the vector map over the raster image,
A shift was observed when the vector file was overlaid with the raster image which was corrected by applying an affine transformation on the raster image. Accuracy values are shown below.

Table 4-a: Translation coordinates and accuracy assessment. Source points were identified by critical examination of the vector file and moved to their corresponding destination points by a translation.

ID	X Source	Y Source	X Destination	Y Destination	Residual Error
1	694616.37998	5853241.04750	694605.30610	5853240.93340	0.01507
2	703565.98251	5852135.21313	703554.98410	5852135.04390	0.01051
3	698983.75381	5848506.38581	698972.69710	5848506.25270	0.01059
4	697804.72306	5855811.29816	697793.66200	5855811.19410	0.01499
RMS Error:	0.012986				

4.1.3. Inconsistencies in data

Whereas it's common in this area for parcels representing the same class to have dissimilar land cover, there are instances where the change was extreme to warrant allocation to a different class. As such the vector map contained parcels whose land cover clearly didn't correspond with the assigned land cover classes and care was taken to not include these areas in the training image.

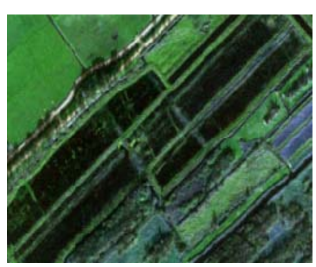

Figure 4-a: Parcels representing the swamp class. Clearly mistaken for grasslands (left) and mistaken for water (right) due to flooding at irrigation. Image is represented as true colour with R, G, B in bands 3, 2 and 1.

4.2. Flow of methodology

The structure of the method adopted followed the sequence shown in Figure 4-b.

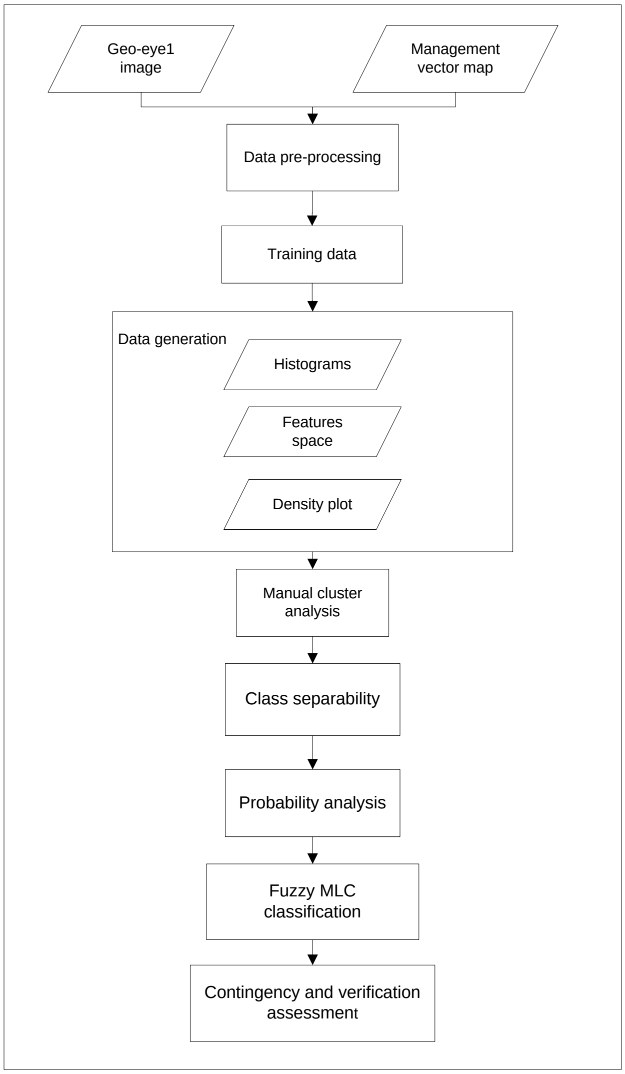

Figure 4-b: Flow of methodology. The processes carried out in this study included training, clustering for subclass generation, analysis of subclasses by class separability and probability images, fuzzy maximum likelihood classification and contingency and verification accuracy assessment by traditional and fuzzy error matrices.

4.3. Training data

The method used to obtain training data in this study is akin to small block training as described in section 2.2. Parcels belonging to a particular class were identified and only pixels wholly contained within these parcels, hereto referred to as pure pixels, were used as training data for that class.

Table 4-b: Number of pure pixels per class that define the training data. Training was constrained to include only pure pixels. Wet soil class has the least number of identified pixels and it's not well represented in the training area.

Reeds	Forest	Grass	Swamp	Wet	Quaking bog	Moist	Water
152703	235588	21967	53783	932	21651	55596	59919

A subset of the image was selected from which training data was sampled. This was chosen such that it contained a reliable number of parcels representing all classes found in the image. By overlaying the raster image with the management map, selection of samples for the classes was restricted to pixels that were fully contained within parcels. This made sure that boundary pixels were not included in the training data. And this in turn guaranteed pure training samples for the classes.
This data was used to explore the properties of the classes which it described. This was done by use of histograms, 2D and 3D feature spaces and density plots. To allow for shorter notation, in diagrams generated during this research, the notation wet (...) and moist (...) was used to denote wet (poor soil and rare plant species) and moist (poor soil and rare plant species) classes respectively.

4.3.1. Histogram generation

Histograms were generated for all classes in all four image bands.

Choosing bin width depended largely on obtaining a smooth display in the data displayed thereafter i.e. avoiding course representation of data and also avoiding sparse representation of bins (as seen in the wet class). Increasing number of bins could lead to noise where as using a number that is too low could lead to coarse representation of the data. Because of the varying number of training pixels obtained per class, different bin widths were used to generate histograms for different classes.

4.3.2. Feature space generation

Feature spaces of data in individual classes were plotted for all four bands. A feature space plot for a combination of all classes in band 3 against 4 was mostly used for analysis as these were bands were more descriptive.

4.3.3. Density plots generation

Feature space plots were improved to display density properties of the data. Density plots could add to understanding of the data. Here also, plots of band 3 and band 4 were mostly used for analysis as they were more descriptive of the data.

4.4. Cluster analysis

From the density plots, clusters were evident in almost all classes. It was therefore required to treat the classes as a super class represented by sub clusters. Clusters were identified from the density plots using a manual clustering procedure implemented in R. The clusters were taken to represent the subclasses present within the super classes.

4.4.1. Cluster identification

Manual cluster analysis was implemented using R software. Clusters were identified using the most significant pair of bands 3 and 4. A threshold of not more than 30,000 pixels per plot was used and the density plot parameters adjusted so as to avoid overshadowing of low density clusters by higher density clusters. The pixels were chosen randomly from total number of pixels identified per class.

Clusters which were taken to represent subclasses were identified from the density plots. The class statistics of these clusters i.e. the mean and covariance, were obtained. Examples of manual cluster identification is shown in the Figures 4-c.

As described in Richards (2013) , when clustering was complete it was investigated to see whether some cluster could be discarded, merged or re-assigned. These decisions were made on the basis of spectral separability and analysis of probability images.

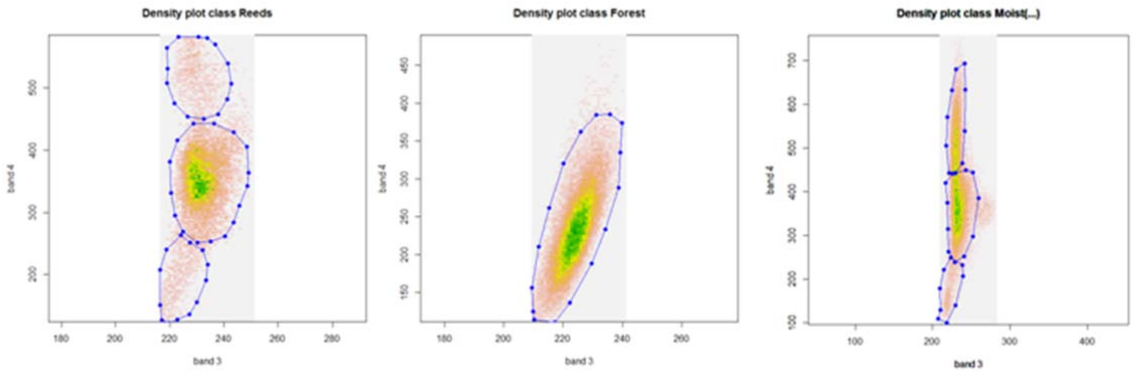

Figure 4-c: Sub-classes identified as clusters by manual delineation. The number of clusters in a plot showed the number of subclasses within that super class. A threshold on the number of pixels displayed per class was applied to enable identification of clusters with lower density.

4.4.2. Class separability

Class separabilities, which were computed using both Transformed Divergence and Jeffries Matusita (as described in Section 2.4, were evaluated comparing each subclass to all other subclasses defined.

4.5. Probability images and fuzzy classification

The classification scheme developed involves the assignment of a parcel to a class according to the following criteria. The probabilities of candidate classes within a pixel are calculated. For all pixels within a parcel, the sum of probabilities belonging to individual classes is obtained. The parcel is then assigned to the class which has the highest sum of probabilities.

Probability is derived as;

$$p(y|w_k) = \exp\left(-\frac{1}{2}(y-\mu_k)^{\mathrm{T}} C_k^{-1}(y-\mu_k)\right) \tag{4.2}$$

4.5.1. Probability images

Conditional probabilities of the subclasses were generated. These were used to plot probability images which were showing the probability of a pixel to belong to a particular subclass. These were normalised and plotted on a scale of minimum 0 and maximum 1 shown by DN values 0 to 255 respectively.

Through combined analysis of proportion class images, probability images, class separations and visual interpretation, the subclasses were sorted for those that were most likely to represent their allocated super class and those that showed high departure from their primary class. A final selection of classes was made involving elimination and re-allocation of the sub classes to the super class which they depicted.

4.5.2. Fuzzy Maximum Likelihood Classification

Pixel based MLC was first carried out on the area using super class statistics i.e. means and covariance of super classes considered as individual classes without subclasses. After sub class identification and analysis, using the final selection of subclasses (as identified in Section 4.5.1), a pixel based MLC was also carried out on the training area and also over a subset of the study area used for verification. This was followed by MLC based object oriented fuzzy classification which involved the following sequence of actions;

1. For each pixel, the probabilities of candidate classes within that pixel were calculated

2. In a parcel, the probability of a class within that parcel was calculated as a sum of probabilities of that class in all pixels contained in that parcel.
3. Memberships of classes within a parcel were then computed as normalized probabilities (equation 4.3) where the possibility of the classes was constricted to range from 0 to 1, for minimum and maximum membership respectively.

Deriving memberships for parcels;
Given that;
k = class, l = parcel; i, j and k are indices of identified entities
$i \in L_l$ = pixel i being inside parcel l
v_{lk} = membership of parcel l in class k
c = constant of normalisation

The membership is computed as follows:

$$v_{lk} = c \sum_{i \in L_l} p_{ik} \tag{4.3}$$

Where;

$$\sum_{k}^{\forall k} v_{lk} = 1; \quad \text{and} \quad c \sum_{k} \sum_{i \in L_l} p_{ik} = 1$$

The output of this fuzzy classification is a series of membership images. A membership image is displayed per class. Memberships of parcels to classes are represented in black for no membership (0) and white for full membership (1). Grey levels display the degree of membership to a class.

4.5.3. Contingency and verification assessment

The accuracy assessment of the classification result was done using confusion matrices for both 'hard' result (by defuzzification i.e. assigning the parcel to the class with the highest membership) and fuzzy result (considering the memberships of all candidate classes). This was applied over the training area to obtain a contingency analysis and also over a different subset of the study area for verification analysis. The confusion matrices returned values for producer accuracy, user accuracy and overall accuracy. The Kappa coefficient was also computed.

The defuzzified result was evaluated using the conventional error matrix while the fuzzy result was evaluated using Fuzzy error matrix (FERM) as described in Binaghi et al. (1999).
The effect of size of parcel was evaluated by comparing results obtained when using those parcels that had at least 5 pixels centred within the parcel and this was compared against parcels with at least 25 pixels centred in the parcel. The final super classes that were assessed in the final classification were 6 in number and were labelled as seen in Table 4-c.

Table 4-c: Final classes considered at classification. 6 classes were considered during classification and the individual super classes are a combination of appropriately re-allocated sub classes.

Sup ID	Superclass
1	reeds
2	forest
3	Grass
4	Quaking bog
5	Moist
6	Water

4.5.4. Generation of misclassification images

To visualise the occurrences of misclassification pertaining to each class, misclassification images were plotted. These show the possibility of true representation of parcels for a particular class and of misclassification to another class.

5. RESULTS

5.1. Training and data generation

The following plots show the proportionality of the super classes within the training site. There is inadequate amount of training pixels for the wet class. Quaking bog and wet classes have low amounts of training data while forests and reeds have the large amounts. Moist and water classes are in the form of narrow parcels and act mostly as separators for the dominant classes. The unclassified parcels show area which isn't assigned any particular land cover on the management map or had land cover not important to this study.

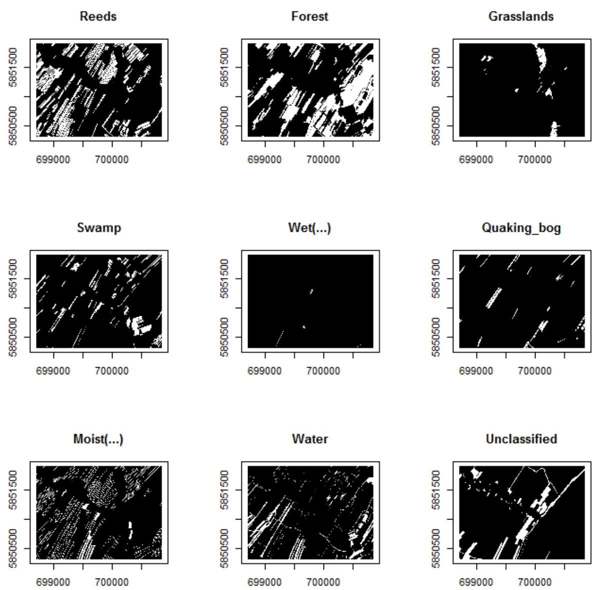

Figure 5-a: Proportion of classes within the training area. Forest and reed lands are most dominant classes in this area and Wet class the least present. Moist and water classes are contained in very narrow parcel in some cases having less than a pixel size in width.

5.1.1. Histograms

Reeds class shows one prominent peak in the first 3 bands and two prominent in band 4, and there is a low shoulder on the left of the histograms in all bands (see Figure 5-b). However there is an elongated tail on the right for all bands which could indicate presence of a class with low mean and wide spread.

Forest class shows one peak in histograms across all the four bands. The grass class shows a varying number of peaks in all bands with up to 4 peaks detected in band 4. The wet class has varying number of peaks depicted in all bands with band 1 showing 3 possible peaks. Water class has one prominent peak with an elongated tail to the right (positively skewed). The moist class shows varying peaks with band 4 depicting 3 peaks. Quaking bog histogram has one prominent peak in all bands and elongated tail to the left in bands 1 and 2. Swamp has one prominent peak in bands 1 to 3, and 4 peaks are suspect in band 4.

The training Histograms for data in all four bands are displayed per class in Figure 5-b.

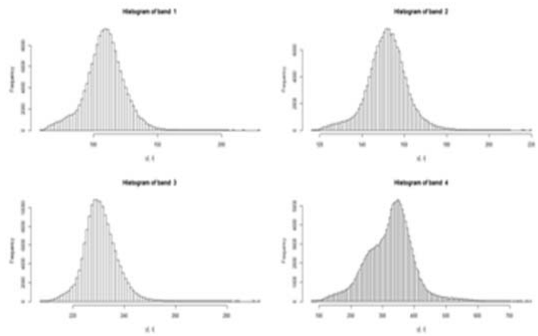

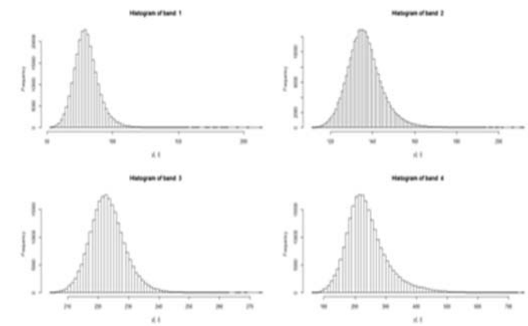

a) Reeds .b) Forest

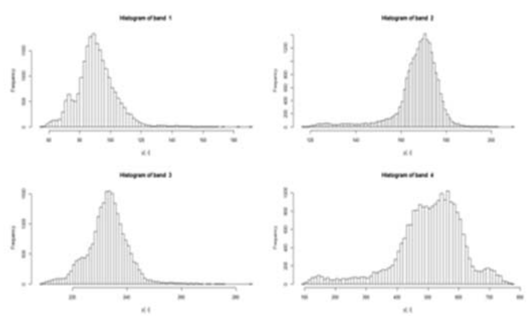

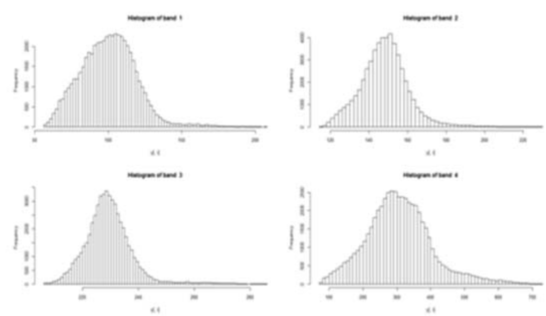

c) Grass .d) Swamp

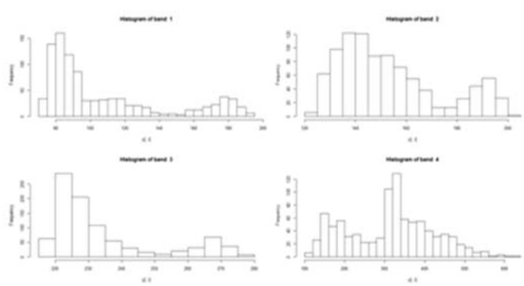

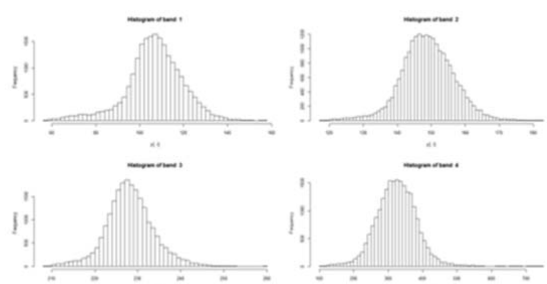

e) Wet .f) Quaking bog

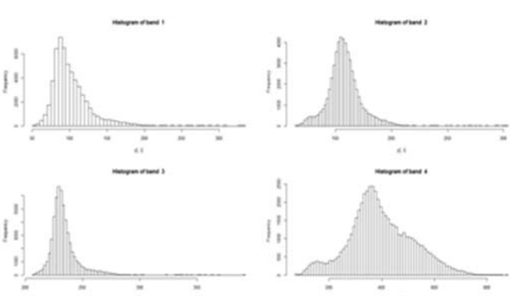

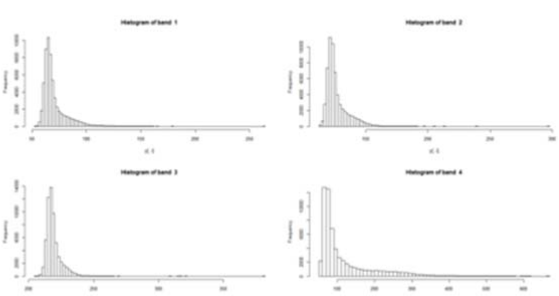

g) Moist h) Water

Figure 5-b: Histograms for all classes displayed for all four bands. Plots of band 3 against 4 are more descriptive of the data in most classes. Multi modality can be seen from the multiple modes and skewed plots. Low training data for wet class results in course representation of the class by histogram.

5.1.2. Feature spaces analysis

The distribution of all classes in feature space is displayed in Figure 5-c for band 3 against 4. It can be seen from extent of distribution and also from the feature space of all classes combined, that almost all classes fall within the same range of values. Only water class has a different distribution with very low values in both bands as compared to the other classes.

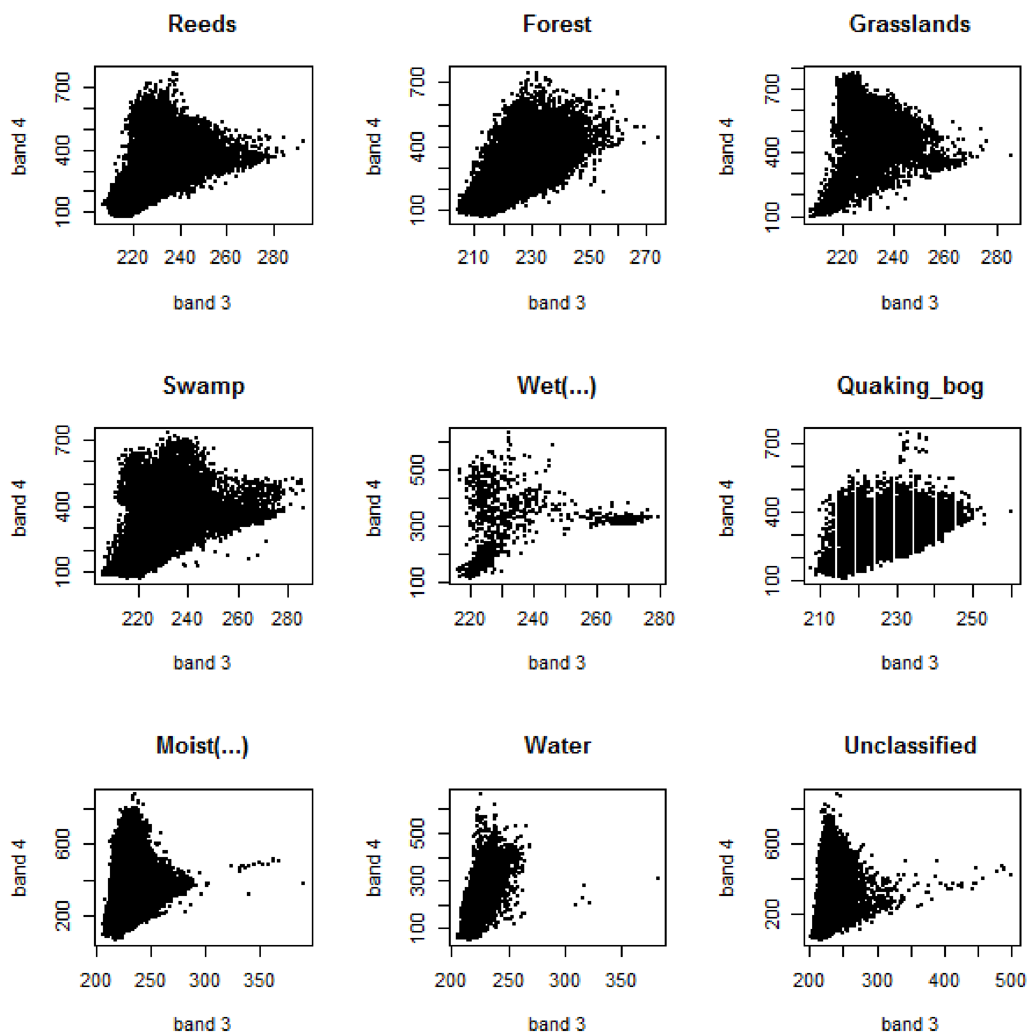

Figure 5-c: Feature space of all classes plotted for band 3 against 4. Multi modality can be identified in several plots most clearly in reeds, grasslands, swamp and moist classes. Wet class has insufficient data for proper identification of clusters. Water has the lowest values in both bands. The other classes which are mostly vegetation cover have high values in both bands as expected. This is characteristic of water and vegetation in red and near infra red spectrum.

5.1.3. Density plots

The density plots show intensity of number of points where green and brown represent highest to lowest density values. From the plots, the peaks observed in the histograms are visible as clusters. Forest and water classes show one cluster in all bands while other classes display varying presence of clusters albeit some with much higher densities than others.

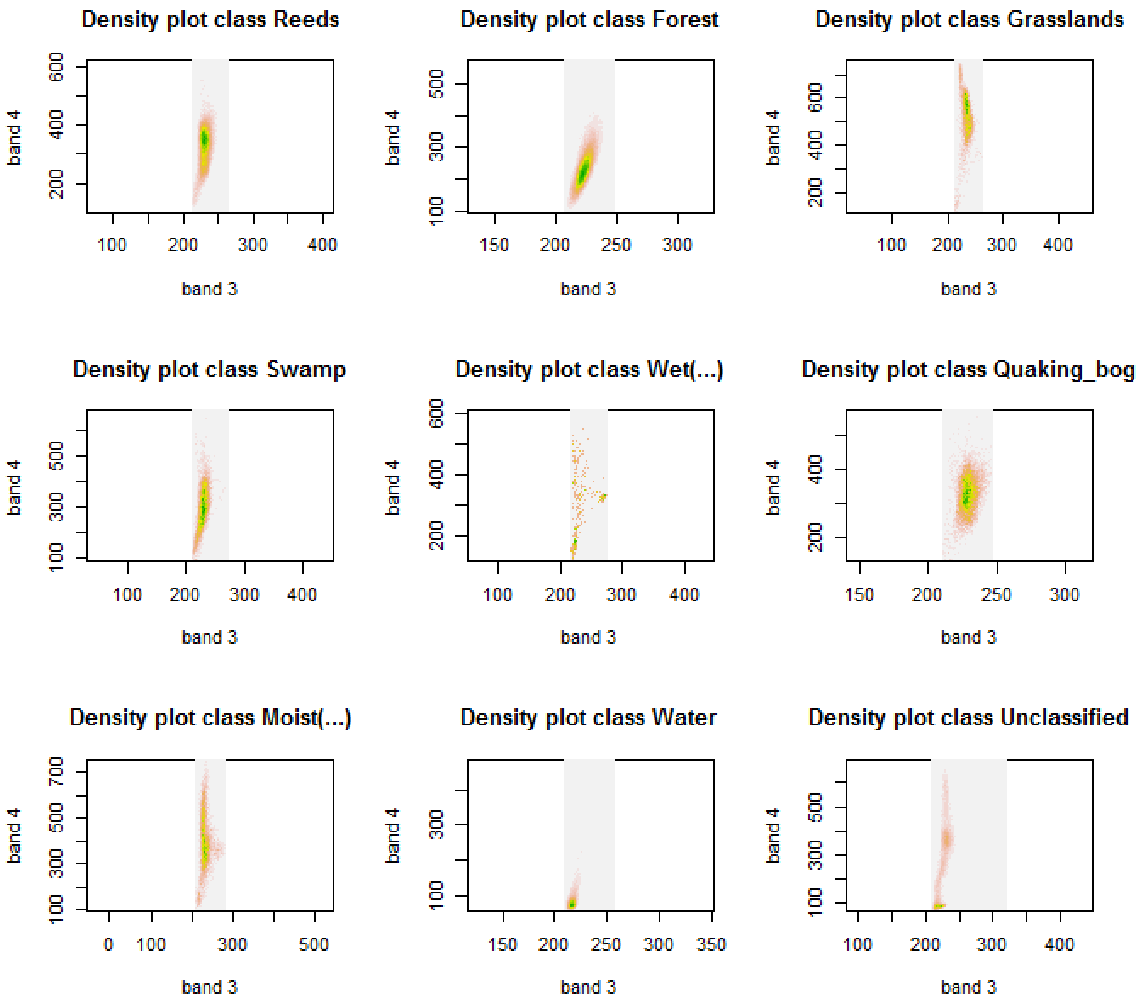

Figure 5-d: Density plots of all classes in band 3 against 4. The colour scale is such that green and brown showing highest to lowest density respectively. All data per class is plotted in band 3 against 4. Clusters can be identified in most classes. Water class plots with the lowest values in band 4 while the others have high values in both bands. The forest class contains a single cluster. The second water subclass is contained in the lower density cluster shown by an elongated spread of points.

5.2. Clustering results

5.2.1. Cluster identification

21 subclasses were identified within the 8 established super-classes. These are distributed as shown in Table 5-a.

Table 5-a: Identified subclasses and their means in band 1 to band 4 as identified using manual cluster analysis. Swamp class contained the most number of subclasses (4) while forest class was a single class.

Subclass	ID	Class	band1	band2	band3	band4
1	r1	Reeds	109.7157	154.9456	230.568	348.5653
2	r2	Reeds	91.79402	143.99907	227.38128	254.2626
3	r3	Reeds	105.9376	163.8269	234.9853	459.2935
4	f	Forest	79.58828	135.78067	223.43947	229.92029
5	g1	Grasslands	99.32835	155.99616	234.6437	316.08818
6	g2	Grasslands	96.91314	173.8263	238.31225	524.02415
7	g3	Grasslands	142.8581	182.0482	256.1183	353.24
8	s1	Swamp	107.3696	154.9059	232.6502	346.0356
9	s2	Swamp	155.9733	184.437	260.9229	343.1611
10	s3	Swamp	78.85241	135.25621	222.00907	203.42774
11	s4	Swamp	96.99442	171.54722	237.62072	588.47181
12	wet1	Wet	82.25674	134.13599	223.65719	177.51053
13	wet2	Wet	85.17855	148.01353	225.1086	439.67354
14	wet3	Wet	101.3996	152.7741	233.0603	303.4465
15	q1	Quaking bog	108.5645	154.1373	228.0815	364.4368
16	q2	Quaking bog	109.9317	149.7494	230.5285	304.8059
17	m1	Moist	132.2396	174.2661	249.5572	370.0755
18	m2	Moist	87.4863	160.9216	230.1051	527.4107
19	m3	Moist	97.31002	145.45678	229.12701	254.32138
20	w1	Water	79.26784	134.75741	223.62924	183.60027
21	w2	Water	67.06135	123.44551	217.38446	81.80477

5.2.2. Class separability

Jeffries-Matusita distance results are displayed in Table 5-b. The values can be seen to range from0 to 2, indicating minimum and maximum separation with the lowest JM value of 0.249628 indicating separation between subclass 10 (swamp) and subclass 21 (water).

Intra class separation is high with subclasses belonging to the same super class displaying high separation. This is apparent in all super classes. However inter class separation is low with subclasses in one super class being easily confused with subclasses in other super classes.

From class separation results, it is seen that;

- Subclasses belonging to the reeds class are more easily confused with subclasses belonging to quaking bog, moist and swamp.
- Forest class has most possibility of confusion with subclasses belonging to reeds,water and swamp classes.
- Grass subclasses have most possibility of confusion with subclasses belonging to moist class.

Table 5-b: Jeffries-Matusita class separability results for 21 subclasses identified. The values range with 0 to 2 for maximum and no separation respectively. Separation is shown by off diagonal values. These values show separation between subclasses on corresponding row and column.

JM	[,1]	[,2]	[,3]	[,4]	[,5]	[,6]	[,7]	[,8]	[,9]	[,10]	[,11]
[1,]	0.00	1.23	1.38	1.86	2.00	2.00	1.88	0.33	1.94	1.78	1.98
[2,]	1.23	0.00	1.52	0.81	2.00	2.00	1.92	0.94	1.95	0.42	1.96
[3,]	1.38	1.52	0.00	1.92	1.91	1.66	1.39	1.00	1.64	1.90	1.32
[4,]	1.86	0.81	1.92	0.00	2.00	2.00	1.99	1.66	1.99	0.56	2.00
[5,]	2.00	2.00	1.91	2.00	0.00	1.89	2.00	2.00	2.00	2.00	1.80
[6,]	2.00	2.00	1.66	2.00	1.89	0.00	1.49	1.97	2.00	2.00	0.93
[7,]	1.88	1.92	1.39	1.99	2.00	1.49	0.00	1.65	2.00	1.99	1.59
[8,]	0.33	0.94	1.00	1.66	2.00	1.97	1.65	0.00	1.91	1.60	1.89
[9,]	1.94	1.95	1.64	1.99	2.00	2.00	2.00	1.91	0.00	1.94	1.99
[10,]	1.78	0.42	1.90	0.56	2.00	2.00	1.99	1.60	1.94	0.00	2.00
[11,]	1.98	1.96	1.32	2.00	1.80	0.93	1.59	1.89	1.99	2.00	0.00
[12,]	1.98	1.03	1.99	1.49	2.00	2.00	2.00	1.94	1.99	1.03	2.00
[13,]	1.69	1.85	1.17	1.86	1.99	1.77	1.66	1.49	2.00	1.89	1.74
[14,]	1.18	0.45	1.22	1.01	2.00	2.00	1.86	0.77	1.70	0.78	1.94
[15,]	0.42	1.50	1.59	1.88	2.00	2.00	1.97	0.90	1.99	1.87	1.99
[16,]	0.62	0.89	1.57	1.52	2.00	2.00	1.97	0.56	1.94	1.40	1.98
[17,]	1.36	1.35	0.79	1.79	2.00	1.96	1.59	1.03	0.75	1.72	1.84
[18,]	1.76	1.84	0.89	1.88	1.84	1.08	1.25	1.54	2.00	1.88	0.77
[19,]	0.94	0.33	1.53	1.07	2.00	2.00	1.96	0.76	1.85	0.50	1.98
[20,]	1.78	0.54	1.81	0.70	2.00	2.00	1.96	1.58	1.95	0.25	1.98
[21,]	2.00	1.78	2.00	1.97	2.00	2.00	2.00	2.00	2.00	1.80	2.00

	[,12]	[,13]	[,14]	[,15]	[,16]	[,17]	[,18]	[,19]	[,20]	[,21]
[1,]	1.98	1.69	1.18	0.42	0.62	1.36	1.76	0.94	1.78	2.00
[2,]	1.03	1.85	0.45	1.50	0.89	1.35	1.84	0.33	0.54	1.78
[3,]	1.99	1.17	1.22	1.59	1.57	0.79	0.89	1.53	1.81	2.00
[4,]	1.49	1.86	1.01	1.88	1.52	1.79	1.88	1.07	0.70	1.97
[5,]	2.00	1.99	2.00	2.00	2.00	2.00	1.84	2.00	2.00	2.00
[6,]	2.00	1.77	2.00	2.00	2.00	1.96	1.08	2.00	2.00	2.00
[7,]	2.00	1.66	1.86	1.97	1.97	1.59	1.25	1.96	1.96	2.00
[8,]	1.94	1.49	0.77	0.90	0.56	1.03	1.54	0.76	1.58	2.00
[9,]	1.99	2.00	1.70	1.99	1.94	0.75	2.00	1.85	1.95	2.00
[10,]	1.03	1.89	0.78	1.87	1.40	1.72	1.88	0.50	0.25	1.80
[11,]	2.00	1.74	1.94	1.99	1.98	1.84	0.77	1.98	1.98	2.00
[12,]	0.00	1.99	1.53	1.99	1.77	1.96	1.98	1.23	1.12	1.84
[13,]	1.99	0.00	1.64	1.76	1.89	1.60	0.77	1.86	1.80	2.00
[14,]	1.53	1.64	0.00	1.53	1.09	0.86	1.70	0.58	0.84	1.96
[15,]	1.99	1.76	1.53	0.00	1.19	1.63	1.86	1.34	1.84	2.00
[16,]	1.77	1.89	1.09	1.19	0.00	1.48	1.91	0.56	1.53	2.00
[17,]	1.96	1.60	0.86	1.63	1.48	0.00	1.57	1.37	1.65	2.00
[18,]	1.98	0.77	1.70	1.86	1.91	1.57	0.00	1.86	1.84	2.00
[19,]	1.23	1.86	0.58	1.34	0.56	1.37	1.86	0.00	0.63	1.81
[20,]	1.12	1.80	0.84	1.84	1.53	1.65	1.84	0.63	0.00	1.58
[21,]	1.84	2.00	1.96	2.00	2.00	2.00	2.00	1.81	1.58	0.00

5.3. Probability images

5.3.1. Conditional probability images

Normalised probility images for the first 9 subclasses are displayed in Figure 5-e.

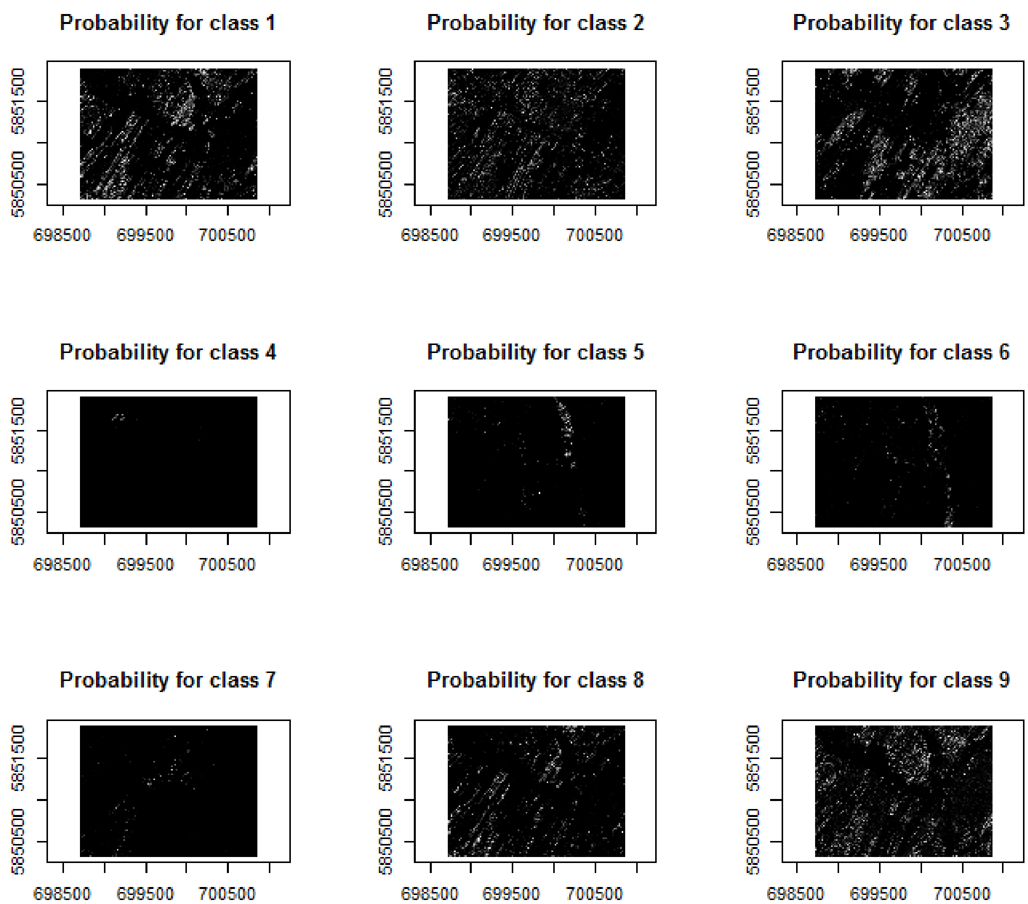

Figure 5-e: Probability images of the first 9 subclasses. Probability to a class is displayed by white and black for maximum and no probability respectively.

5.3.2. Interpretation of subclasses

Confusion in land cover spectral properties for different classes can be seen in the images captured of the area (as shown in Figures 5-f to 5-n).

The subclasses, from analysis of class separation values, comparison with proportionality images and management map combined with visual interpretation of the raster image can be described as follows.

1. Reeds:

Subclass 1; r1

This subclass accurately represents the reeds class. However it also classifies parcels covered by quaking bog and moist class that have similar land cover.

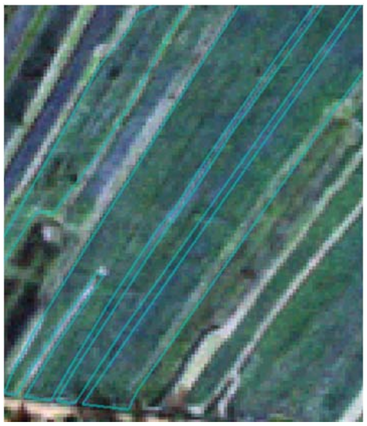

Figure 5-f: Images showing an instance of subclass r1. This land cover is found to be similar with that found on some quaking bog parcels.

Subclass 2:r2

This subclass is poorly representative of the reed class as it equally classifies the forest class as well. This is because of parcels classified as reeds which contain forest class and those that are overshadowed by the tree canopy.

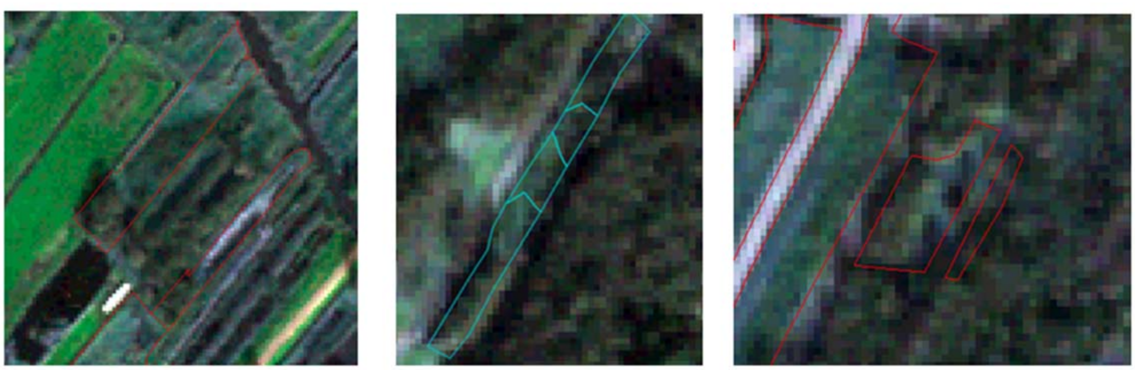

Figure 5-g: Images showing instances of subclass r2. Narrow reed land parcels neighbouring forest parcels are affected almost completely by canopy. In other cases trees are present on the parcel.

Subclass 3: r3

This class is averagely representative of reeds class with an equal chance of being classified as moist class and a few parcels of the swamp class due to common land cover.

Figure 5-h: Image showing an instance of subclass r3. This land cover is also found on moist and swamp parcels hence the confusion between the closely related subclasses.

2. Forest: f

The forest class is represented by one major class and no subclasses and this class accurately represents the forest land cover in the image.

3. Grasslands;

Subclass 5; g1
This subclass is highly representative of the grass class in the general overview; it captures those parcels labelled as grass which have high spectral values.

Subclass 6; g2
This subclass is highly representative of the grass class. With almost negligible occurrences of misclassification in those areas whose land cover is similar to grass.

Subclass 7; g3
This subclass is highly representative of the grass class in the general overview; it captures those parcels labelled as grass which have lower spectral values and may also classify some moist parcels which have similar spectral properties.

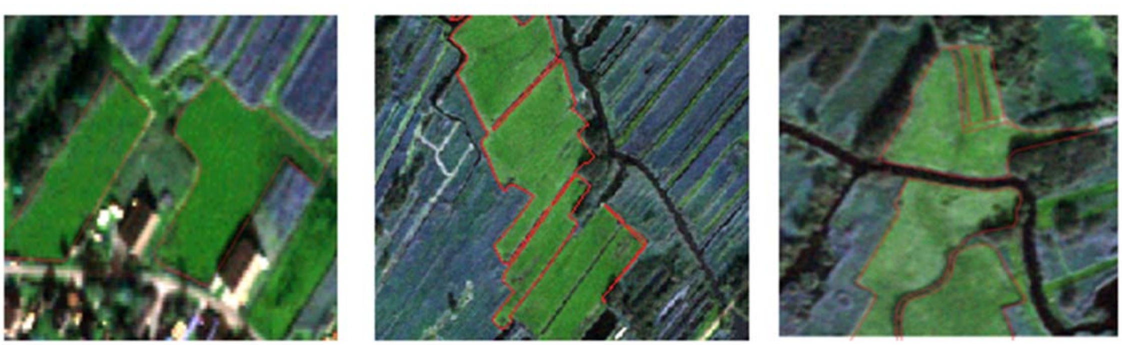

Figure 5-i: Images showing instances of subclasses g1, g2 and g3 (L-R) respectively. The different intensities of land cover spectra shown in the different subclasses could be due to different stages of growth and results in identification of separate subclasses representing the same class.

4. Swamp

Subclass 8; s1

This subclass is representative of some swamp parcels, also highly representative of reeds and quaking bog.

Subclass 9; s2

This subclass is representative of only a couple of swamp parcels, and then generally representing some of the moist class. It represents swamp and moist class parcels which share common land cover. And on the whole it contains very few classified pixels.

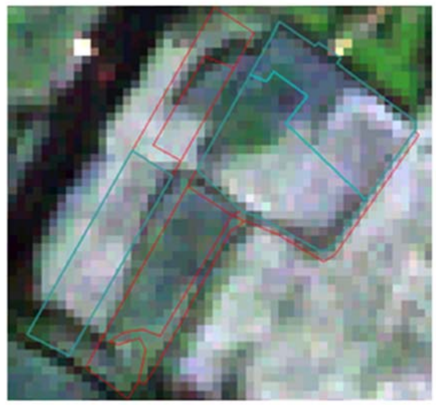

Figure 5-j: Images showing instances of subclasses s1 and s2 (L-R) respectively. These two subclasses are easily confused with reeds, moist and quaking bog classes because of similar land cover.

Subclass 10; s3

This subclass is highly misrepresentative of the swamp class over all and it’s a more general representation of the forest class. It however captures those parcels labelled swamp which have high number of trees.

Subclass 11; s4

This subclass is highly misrepresentative of swamp on the whole but accurately represents grasslands. This is due to a swamp parcel with grass land cover.

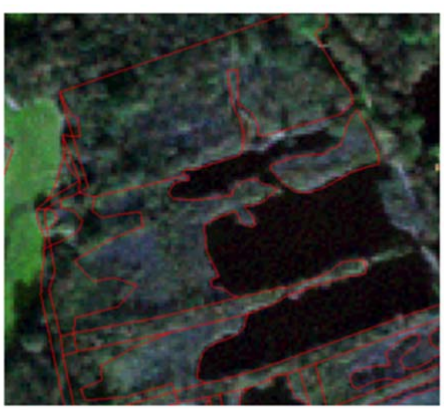

Figure 5-k: Images showing instances of subclasses s3 and s4 (L-R) respectively. Swamp parcels contain multiple land cover which is dominant in other classes.

5. Wet; this class has insufficient number of training pixels and therefore class statistics aren't true depiction of the class. However the subclasses that were identified can be described as follows.

Subclass 12; wet 1 and Subclass 13; wet 2 are generally representative of moist class.
Subclass 14; wet 3 is more representative of reed land and moist classes

6. Quaking bog

Subclass 15; q1
This is a true representative of some of the quaking bog parcels. However it also classifies those reed parcels that have similar land cover to the identified quaking bog parcels.
Subclass 16; q2
This subclass is good representation of most quaking bog parcels. But it also classifies a great number of parcels of reeds and swamp which share similar land cover.

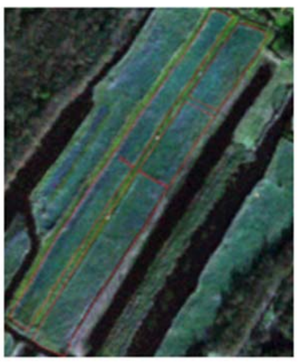

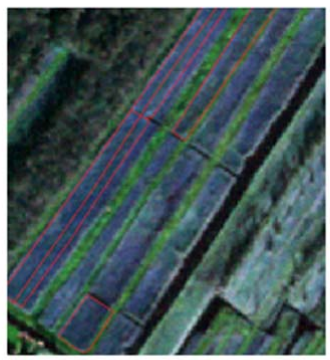

Figure 5-l: Images showing instances of subclasses q1 and q2 respectively. These have similar land cover to reeds and moist subclasses.

7. Moist

Subclass 17; m1
This is a good representation of moist class. However it also classifies a considerable number of parcels belonging to reeds and swamp classes.

Subclass 18; m2
This classifies both moist and grasslands. This is because some moist parcels have similar land cover to grassland parcels.

Subclass 19; m3
This subclass also classifies the forest class. The moist class parcels which are represented by this subclass are mostly those which are overshadowed by the tree canopy.

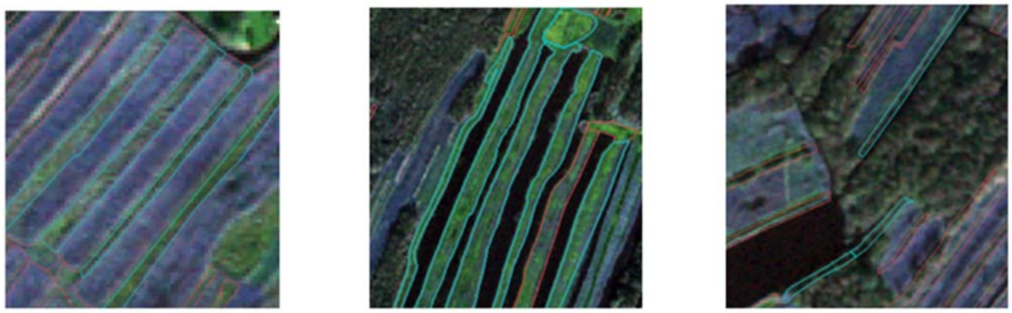

Figure 5-m: Images displaying instances of subclasses m1, m2 and m3 respectively. Moist parcels are very similar to reeds, quaking bog and grass subclasses due to similar land cover. They are also easily mistaken for forest due overshadowing by canopy.

8. Water

Subclass 20; w1

This subclass classifies both water and forest. However it's more representative of forest and water bodies that have higher values, presumably shallow water and water overshadowed by tree canopy.

This subclass maybe due to inclusion of a parcel which is part of management type 'cages for catching ducks'. This management type was merged with other water types. Whereas all other parcels in this type have water, this particular parcel has different land cover. Confusion in this subclass can also be attributed to narrow water ways which are overshadowed by tree canopy.

Subclass 21; w2

This is good representation of the water class. However some of the smaller water ways aren't classified.

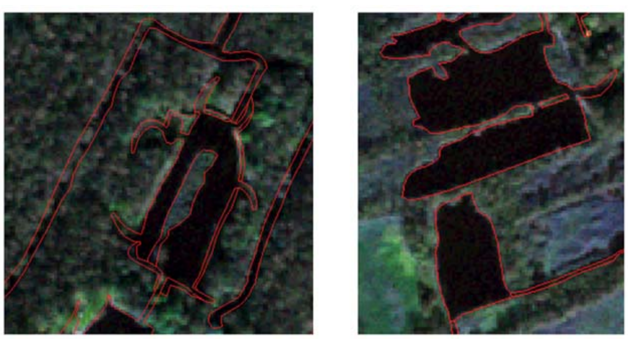

Figure 5-n: Images displaying instances of subclasses w1 and w2 respectively. Narrow water ways next to forest parcels are greatly affected by canopy. Larger water bodies are accurately represented.

In consideration of the above, the original 21 subclasses were edited and re-evaluated as follows;

Subclasses 7 and 9 were allocated to the moist class, subclass 11 to the grass class and classes 2, 5, 8,10,12,13,14,17,19 and 20 were eliminated. The selected subclasses were assigned as shown in Table 5-c. The wet class was eliminated due to insufficient training data. The swamp class was eliminated as it cannot be distinguished as a unique land cover type because the land cover on these parcels is a combination of already established classes. Priority was given to reed lands where the subclass which showed equal possibility of belonging to reed lands and quaking bog class was allocated to reed lands.

Table 5-c: Subclasses selected from initial subclasses. These are more descriptive of their allocated super class.

sub ID	Subclass	Allocated super class	Sup ID
1	r1	reeds	1
2	r3	reeds	1
3	f	forest	2
4	g1	grass	3
5	g2	grass	3
6	g3	grass	3
7	s2	moist	7
8	q1	quaking bog	6
9	q2	reeds	1
10	m2	moist	7
11	w2	water	8

5.4. Fuzzy classification (Membership images).

Membership images are displayed in Figure 5-o. Membership 1 and 0 are displayed as white and black respectively. The grey tones display the degree of membership to the class. Membership to subclasses of grasslands, forest and water is high. The membership of second subclass representing reeds is low compared to the other two subclasses which display moderate membership. Also membership to quaking bog is moderate and membership to moist class is low.

5.5. Contingency and verification analysis.

Table 5-d shows accuracy results for pixel based MLC and contingency analysis of crisp result and fuzzy result using threshold of a minimum of 5 pixel centres in a parcel. The accuracy of the fuzzy maximum classification was assessed both as a crisp result using conventional error matrix and also as fuzzy result using FERM. A summary of the contingency and verification analysis results are displayed in Table 5-e.

Super class Pixel based MLC had overall accuracy of 54.17% while Sub- class Pixel based MLC had overall accuracy of 68.04%. This was a 14% increase in accuracy which showed that considering subclasses for this data improved results.

Contingency analysis results show moderate accuracy with kappa values above 0.4 for crisp classification; however the accuracy is lower with fuzzy classification. There is exception of quaking bog and moist classes which show an increase in producer accuracy with fuzzy classification. Lowest accuracies are seen for quaking bog and moist classes while highest accuracies are seen for the forest class. Reeds, grasslands and water classes show moderate accuracies. In general, water, quaking bog and moist classes have higher user accuracy compared to the producer accuracy whereas reeds, forest and grassland classes have higher producer accuracy compared to the user accuracy.

Comparing result for larger parcels, slight increase is seen in the overall accuracy; however there is a decrease in kappa value.

5.6. Misclassification images.

Figure 5-q shows some of the misclassification images produced post classification. Positively classified parcels are green whereas misclassified parcels are red. Reeds are mostly misclassified to quaking bog, forest and moist classes in that order with a few parcels misclassified to water class. Overall forest and grassland classes have few misclassifications. Quaking bog is mostly misclassified as reed land and on a smaller scale as moist. Moist class is moderately misclassified to reed land and grassland. Water has highest misclassification in forest class.

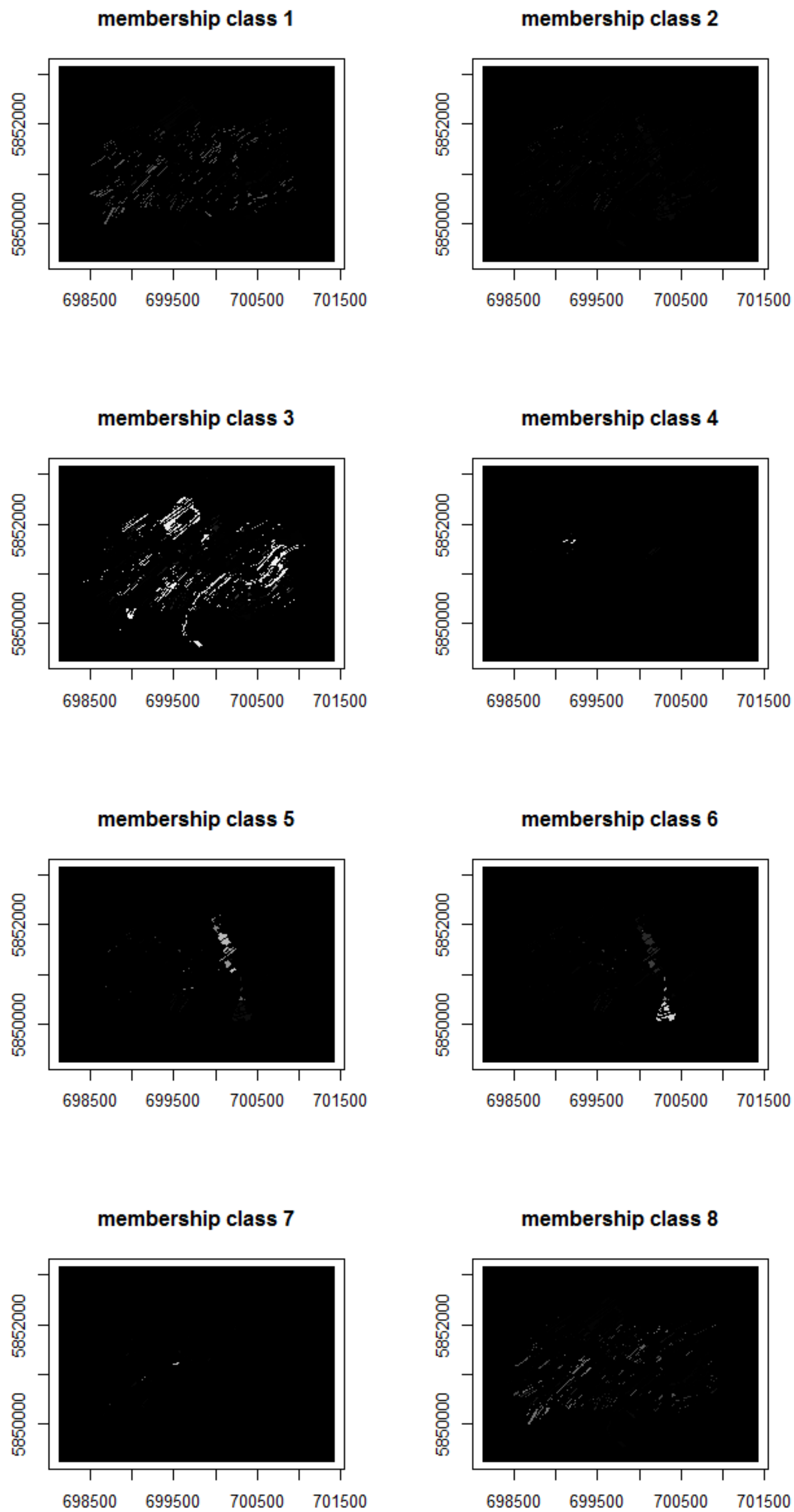

Figure 5-o: Membership images for first 8 subclasses. White and black colour values are indicative of maximum and minimum membership respectively. Forest and grassland display highest membership to their subclasses.

Table 5-d: Pixel based MLC accuracy (top), parcel based Contingency analysis Tables for crisp (defuzzified) result (middle) and FERM for the fuzzy result (bottom); for threshold of 5 pixels per parcel.

	Reeds	Forest	Grass	Q.bog	Moist	Water	Total	Error of commission%	User accuracy%
Reeds	121954	19291	1310	16702	39333	7121	205711	40.72	59.28
Forest	15150	221702	1462	1472	11502	19134	270422	18.02	81.98
Grass	1228	844	18723	141	7265	211	28412	34.10	65.90
Q.bog	33091	4051	16	6968	5308	267	49701	85.98	14.02
Moist	7464	7404	2025	885	25610	1741	45129	43.25	56.75
Water	562	919	19	3	479	44451	46433	4.27	95.73
Total	179449	254211	23555	26171	89497	72925	645808		
Error of ommission%	32.04	12.79	20.51	73.38	71.38	39.05			
Producer accuracy%	67.96	87.21	79.49	26.62	28.62	60.95		Overall accuracy%	68.04

	Reeds	Forest	Grass	Q.bog	Moist	Water	Total	Error of commission%	User accuracy%
Reeds	315	18	2	61	226	37	659	52.20	47.80
Forest	58	601	5	5	82	41	792	24.12	75.88
Grass	1	1	21	0	41	4	68	69.12	30.88
Q.bog	12	0	0	5	10	0	27	81.48	18.52
Moist	10	3	0	1	56	2	72	22.22	77.78
Water	5	4	0	0	5	59	73	19.18	80.82
Total	401	627	28	72	420	143	1691		
Error of ommission%	21.45	4.15	25.00	93.06	86.67	58.74			
Producer accuracy%	78.55	95.85	75.00	6.94	13.33	41.26		Overall accuracy%	62.51
Kappa coeffecient = 0.45467									

	Reeds	Forest	Grass	Q.bog	Moist	Water	Total	Error of commission%	User accuracy%
Reeds	242.05	56.783	3.3152	49.165	192.1	35.948	579.412	58.22	41.78
Forest	64.623	541.32	5.364	6.9887	80.21	41.156	739.664	26.82	73.18
Grass	5.7895	3.1498	16.876	0.1867	39.3	3.7023	69.0072	75.54	24.46
Q.bog	71.515	10.904	0.1394	14.333	41.79	3.5214	142.205	89.92	10.08
Moist	12.081	7.8955	2.2138	1.3169	60.19	3.6704	87.371	31.11	68.89
Water	4.9402	6.9454	0.0915	0.0098	6.351	55.002	73.3398	25.00	75.00
Total	401	627	28	72	420	143	1691		
Error of ommission%	39.64	13.66	39.73	80.09	85.67	61.54			
Producer accuracy%	60.36	86.34	60.27	19.91	14.33	38.46		Overall accuracy%	54.98
Kappa coeffecient = 0.3723057									

Table 5-e: Summary of accuracy results obtained in both crisp and fuzzy assessment for thresholds of 5 and 25 pixels per parcel. Reeds, forest and water classes have the highest producer accuracy while water has higher user accuracy. Accuracy of fuzzy result is generally lower than that of crisp result.

	Crisp								**Fuzzy**							
	Contigency				Verification				Contigency				Verification			
	>5 pix/parcel		>25 pix/parcel		>5 pix/parcel		>25 pix/parcel		>5 pix/parcel		>25 pix/parcel		>5 pix/parcel		>25 pix/parcel	
Class	p.a	u.a	p.a	u.a	p.a	u.a	p.a	u.a	p.a	u.a	p.a	u.a	p.a	u.a	p.a	u.a
Reeds	78.55	47.80	80.32	50.40	71.11	29.36	72.50	33.72	60.36	41.78	60.52	44.30	57.42	26.12	60.06	30.70
Forest	95.85	75.88	98.26	78.88	94.78	72.19	100.00	72.57	86.34	73.18	88.48	75.66	86.86	71.21	91.67	71.86
Grass	75.00	30.88	88.24	32.61	87.50	38.89	100.00	46.67	60.27	24.46	72.04	24.27	57.34	26.26	63.15	34.71
Q.bog	6.94	18.52	7.27	19.05	6.45	25.00	3.57	16.67	19.91	10.08	21.08	10.34	21.97	24.97	20.75	27.71
Moist	13.33	77.78	14.38	78.95	12.94	57.89	12.70	72.73	14.33	68.89	15.20	70.53	14.82	57.65	16.16	67.34
Water	41.26	80.82	51.06	82.76	31.25	90.91	42.11	100.00	38.46	75.00	47.04	77.02	28.37	88.92	37.67	97.46
o.a	62.51		65.09		54.11		56.49		54.98		56.87		50.25		53.04	
Kappa	0.4547		0.42055		0.3746		0.3625		0.3723		0.3484		0.4769		0.3315	

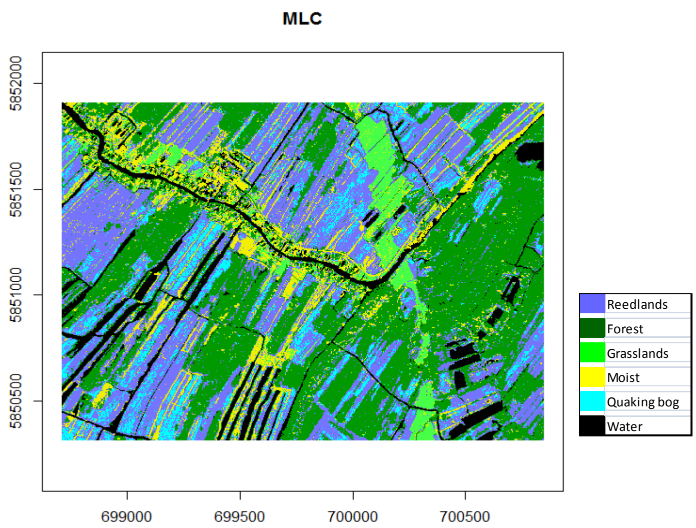

Figure 5-p: Sub class Pixel based maximum likelihood classification of training site using final subclasses. Forest class has highest classification accuracy.

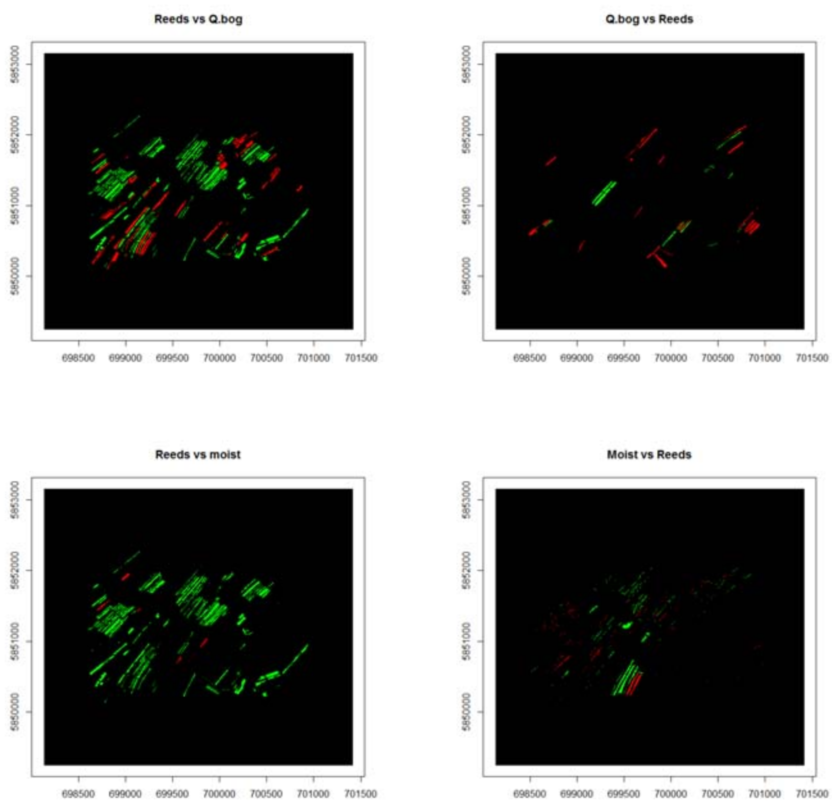

Figure 5-q: visualisation of selected classes showing misclassification. Where Reeds Vs Q.bog displays positively identified reed parcels (green) and reed parcels misclassified as Q.bog (red). Quaking bog is highly misclassified as reed lands.

6. DISCUSSION

6.1. Training and data generated

6.1.1. Histograms

Training data was dependent on the management map for prior information about land cover in this area. Whereas all the other classes had adequate number of training pixels identified, class 5 (wet) didn't have enough training pixels to define the properties of that class as seen in the class 5 histogram where due to an inadequate number of training pixels for that class, there is coarse representation of data distribution.

Inspection of the histograms shows intra class variability present within all the defined land cover classes except class 2, the forest class. This can be seen in the histograms which show evidence of multimodality within the classes by displaying various modes for the data. This is most obvious in histograms of band 4 for reeds, grasslands and moist classes.

It can be seen that while in some bands, the data showed a tendency towards unimodality, in another combination of bands it showed presence of sub classes (e.g. in the reeds class, histogram of band 3 shows unimodal distribution, but that of band 4 shows 3 underlying distributions).

Although the water class show one major cluster, the multimodality within this class is seen by the extreme skewness of the histogram with the lower end tail denoting the shallow water subclass.

6.1.2. Feature spaces

The feature spaces show that the classes are distributed within the same range of values except for water class which displays very low values in all bands. It's possible to discern intra class variability in all super classes except for class 2 and class 8. This can be seen in Figure 5-c.

Although the class forest displayed unimodality, it's quite probable that there is an underlying class (shadow) contained within the major canopy which isn't displayed due to its nearness in mean to the canopy pixel values and is therefore contained within the distribution.

6.1.3. Density plots

Also the multimodality is evidenced in the density plots where subclasses are present as clearly distinguishable clusters as seen in Figure 5-d. Identification of sub classes as clusters is however dependent on the clustering density. Density plots were plotted with threshold of amount of data to avoid having those classes which have lower density from being overshadowed by the densely represented ones. This can be seen in the reeds and quaking bog density plot, manual cluster delineation was done using density plots generated with a threshold of 30,000 pixels per super class.

In instance where the density is set too high, those classes that are contained within low number of training pixels will be ignored. This can be seen in by comparing corresponding scatter plots for Reeds class in Figure 5-d and Figure 4-c. This therefore requires proper interpretation to correct for ignoring of present classes which can be overshadowed by higher density data. This explains why even though the

number of occurrence in the density plots for some of the identified sub classes is low, they are necessary and require recognition as subclasses.
The sub classes that are identified as being depicted by longer tails on the distributions are those classes which have close means but have high standard deviation.

6.2. Clustering and subclass identification

6.2.1. Subclass identification

"Due to multimodality present a single Gaussian at class level is inadequate to capture the distribution of the data" (Ju et al., 2003).
Due to multimodality observed from the histogram and scatter plots, classes are treated as super classes which are composed of one or more normally distributed sub classes.
The number of underlying subclasses was chosen considering both the histogram representation and also the density plots of the data in all four bands.

Following the above criteria, the 8 super classes were represented by a total of 21 subclasses as defined in Table 5-a.

6.2.2. Class separability

Since these land covers are generally characterized by vegetation, they are more distinguishable in bands 3 and 4 the red and near infra red bands and not so much in band 1 and 2 the blue and green bands. However their representation in band 4 and 3 is not good enough to set them apart from each other clearly (as seen from the plots). Hence class separability analysis provides clearer insight into the nature of these subclasses.

Class separability analysis is essential in discriminating among closely related spectral signatures. Using the class separability measures of TD and JM (Table 5-b), separabilities were computed for all subclasses.
Several subclasses have very low separability values and as such are almost identical in feature space. This could show that they share a super class.

6.3. Probability images

Generating probability images for the subclasses display the probability of all the pixels in the image to belong to that sub class. The possibility of mistaking one subclass for another, which had been displayed in the class separation analysis, can be further observed in these images.
Combined with visual interpretation of the corresponding parcels with these results, it can be seen that instances of correlation between classes occur when the cover on ground is the same. This can be seen in the parcel id 221, where sub class in grass is seen to correlate with moist class.

6.4. Interpretation of subclasses

The subclasses were reallocated as shown in Table 5-c and the wet class was eliminated due to insufficient training data whereas the swamp class was eliminated as it cannot be distinguished as a unique land cover type. In this case, it could be that due to the purpose of the management map, parcels were assigned labels not only according to their land cover but in some cases also the land use.

6.5. Accuracy assessment

Pixel based MLC using selected subclasses outperforms traditional MLC by 14%. This shows that converting multimodal classes into subclasses helped improve the classification of the image and is therefore a reliable approach to improve mapping of poorly separable land cover classes. However improved MLC performs better than fuzzy classification by 5%. This could be partially attributed to using fuzzy classification without appropriate reference data. The use of fuzzy classification in classification of this area returns moderate to poor results for different classes. From using different size of parcels, it is seen that size of parcel has little influence on the accuracy, as it only increases by approximately 3% in both crisp and fuzzy results; as such parcel size isn't a major factor in this assessment.

Crisp accuracy is higher than fuzzy accuracy for all classes except quaking bog and moist, which although have poor accuracies, show a slight improvement in producer accuracy when fuzziness is considered. The very low accuracies of quaking bog are due to its similarity with reed lands which leads to misclassification of most quaking bog parcels as reed land parcels. The low accuracy of moist class is due to its spectral similarity with reed lands and grass land classes which causes many moist parcels to be misclassified as reeds and grass classes. The increase in accuracy in quaking bog and moist parcels could be attributed to the consideration of their membership to reeds class and reeds and grass classes respectively.

The failure of fuzzy classification to display improvement in classification could be attributed to the fact that crisp reference data was used define land cover which is fuzzy in nature. Fuzzy reference data would be preferred for analysis using fuzzy classification. The depiction of higher accuracies by crisp classification could be attributed to the use of crisp reference data in classifying the defuzzified result.

Although overall accuracy is low, the method is able to identify some of the individual classes to a reasonable degree. Foremost are the Forest class parcels, which have very little incidence of misclassification. Reed land, grass and water bodies are also correctly classified with moderate results.

6.6. Summary of observation

Failure to distinguish between some quaking bog and reed lands subclasses can be seen to be due to the spectral similarity of their land cover. The reed lands have been noted as containing sphagnum and wet heath, and sphagnum is also common to quaking bog. Therefore in instances where reed lands have been mowed, it can be expected that there is little difference between land cover on parcels containing the two classes. The presence of reeds among other vegetation cover in this area also brings about confusion especially in cases where the reeds occupy a big proportion of the parcel land cover. Also confusion arises in cases where reeds have grown on the quaking bog parcels.

Confusion in land cover spectral properties due to influence of tree canopy is evident in most classes. This can be attributed to the fact that whereas the management map was compiled from aerial photographs captured in late December, a time when most trees have shed their leafage, the satellite image used in this study is of October. Therefore those parcels which are adjacent to the parcels with forest class, though clearly discernible in the management map, are affected by canopy as seen in the image. This is especially extreme in narrow parcels e.g. water ways. Parcels that are misclassified as water can be seen to be those that have high effect of shadow which shares spectral similarities with water and parcels that are misclassified as forest are those that have been overshadowed by canopy of trees from neighbouring parcels with forest class.

Whereas the used Geo-eye-1 image has capabilities to distinguish vegetation, classes such as water, moist , swamp and quaking bog which have high amounts of moisture content could be better captured by thermal or radar remote sensing images and these types of images also have the capacity to overcome overshadowing of other classes by the forest canopy. Although the resolution of Geo-eye-1 images is high compared to other sensors such as LandSat, it is still not adequate for this study area which has small parcels. Some parcels are very narrow and as a result are completely made up of mixed boundary pixels.

As with all natural land cover, it is important to account for spatial dependence of neighbouring pixels in classification. Object based classification used in this study accounts for spatial correlation between neighbouring pixels through the summing up of probabilities within a parcel. Through this, there is greater influence on pixels within a parcel by surrounding pixels than those far away and hence a higher chance of proper classification. In this study, object based classification also reduces influence of displacement of boundaries from geo-referencing of vector file. By distributing the error found in the boundary pixels over all pixels within the parcel, it effect on classification is reduced.

The accuracy assessment in this study suffers from inappropriate reference data. The reference data depends on the management map which was made to show management classes. These classes don't necessarily correspond to land cover found on the parcels and confusion arises when two or more management classes have the same land cover on the image. Whereas this could be mostly attributed to the management practices in the area, it could to an extent also be due to using a satellite image captured in October 2011and reference map which was compiled using images captured on December 2008 and updated with field data collected up to December 2012. This has an impact in this area as most land cover classes have vegetation which is affected by seasonality. Moreover the management classes are provided as crisp classes with a parcel assigned to one class, although during observation in the field the parcel could have resemblance to more than one class. This affects accuracy assessment of fuzzy classification which should be done using fuzzy ground data as well as fuzzy output.

In spite of the relatively low overall accuracy attained by fuzzy maximum likelihood classification approach used in this study, it is able to clearly identify some of the land cover classes in this area most especially Forest, Grasslands and Reed lands. It can also be anticipated that using more appropriate and accurate ground data will produce classified images with even higher accuracy. More so in defining memberships of a parcel to a class, this method is able to define land cover composition present on parcels. In this study, the retrieved information from the classes more accurately identified for example Forest, Grassland and Reed land could be used by the nature organisation to assist in management decisions especially aimed at developing various habitats which requires specific land cover mixtures. Thus for areas that are being groomed to be habitats for various rare animal species, their extent and the transition from current management class to required land cover composition for areas still being developed could be monitored.

All in all, this method is to an extent able to successfully classify a satellite image for mapping of heterogeneous and poorly separable land cover classes. This is because it provides an appropriate training method which eliminates mixed pixels in training data by using vector overlay of boundary information to obtain pure training pixels. It also overcomes complications brought about by multimodal data through subclass identification which makes the data suitable for use with probability based theory and using fuzzy classification to define memberships of parcels to a class helps deal with fuzzy boundary between classes.

7. CONCLUSION AND RECOMMENDATION

7.1. Conclusion

This research used fuzzy classification of a Geo-eye-1 image in mapping reed lands, a procedure which provides information for management of the area.

The main objective of this research was to define a method for classification of areas with land cover classes which are poorly separable and have high intra class variability.

8 major land cover classes were identified from the management map provided of the area. These included Reed lands, Forest, Grasslands, Swamp, Wet soil, Quaking bog, moist soil and Water. Investigation of the data distribution of these classes was done using histograms, feature spaces and density plots. The classes were seen to have multimodal distribution and they were consequently reduced to subclasses of unimodal distribution through manual clustering.

Class separability analysis of the subclasses and comparison of probability images were used as basis to define allocation of final sub classes and these were then used in classification. Fuzzy maximum likelihood classification was used because of apparent heterogeneity of the land cover classes. The result was displayed as a series of membership images per subclass. Contingency analysis was done by assessing accuracy over training area and also verification was carried out on a different section of the study area. Accuracy assessment of the result was done for crisp (defuzzified) result, using conventional error matrix and for fuzzy result, using a fuzzy error matrix.

MLC using subclasses produced higher accuracy (by 14%) than MLC using individual super classes. This shows a positive impact of remedying multimodality through identification of underlying unimodal distributions thereby improving classification of images for heterogeneous and poorly separable classes.

Overall accuracy of contingency analysis reduced from 62.51 for crisp result to 54.98 for fuzzy result while the kappa coefficient reduced from 0.4547 for crisp result to 0.3732. Accuracies obtained for fuzzy result were lower than corresponding accuracies for crisp results with the exception of quaking bog and moist class which showed an increase in producer accuracy. Accuracies obtained in verification were generally lower than those obtained in contingency analysis but they display similar changes for crisp result and fuzzy result.

The overall poor result of applying fuzzy classification of the Geo-eye-1 image for mapping the reed fields can partially be attributed to the discrepancy between reference data as given by the management map and the land cover displayed in the image. This is because the management map provides management types which are directly translated into land cover classes for use as reference data and also because of the different dates at which the image was captured and the management map compiled. The poor result of fuzzy classification can also be attributed to use of crisp reference data in accuracy assessment of the fuzzy error matrix.

Therefore with adequate reference data, the fuzzy maximum likelihood approach used in this study will be able to provide classified images of better accuracy. The parcel based approach to classification makes it possible to show degrees of correspondence to certain management types, an important requirement in the management of this area which deals with maintaining habitats for rare species. This method also provides the possibility to show parcels where confusion of land cover is greatest.

From consideration of the above, fuzzy maximum likelihood classification of remote sensing images for mapping heterogeneous and poorly separable land cover can be applicable and to an extent provides valuable information which can assist in management of areas so characterised. On its own however, this method provides limited information. Therefore although remote sensing does provide insight into mapping reed fields, at this stage, relying entirely on classification of these images would prove ineffective and other data provided by the current monitoring methods such as field work and aerial photography is still required to support this.

7.2. Recommendations

To improve on classification result obtained by using fuzzy classification in this area, the following is recommended for further research;

- Reference data which corresponds to image used in both date and depiction of fuzzy classes is required.
- This study would benefit from using higher resolution images which would control the number of mixed pixels, a problem faced in many of the parcels.
- Using multi temporal images would also assist in better identification of the different vegetation classes found in this area. Multi temporal analysis could also reduce the effect that overshadowing by tree canopy has on neighbouring parcels.
- Using thermal and/or radar images would support monitoring of parcels which rely on regularised moisture content such as the moist class parcels and swamps.
- Whereas shadow wasn't a major factor in this study, correction for effect of shadow would provide higher accuracy in classification.

LIST OF REFERENCES

Ardila, J. P., Tolpekin, V. A., Bijker, W., & Stein, A. (2011). Markov-random-field-based super-resolution mapping for identification of urban trees in VHR images. *ISPRS Journal of Photogrammetry and Remote Sensing, 66*(6), 762-775. doi: http://dx.doi.org/10.1016/j.isprsjprs.2011.08.002

Arzandeh, S., & Wang, J. F. (2003). Monitoring the change of Phragmites distribution using satellite data. *Canadian Journal of Remote Sensing, 29*(1), 24-35.

Asaeda, T., & Karunaratne, S. (2000). Dynamic modeling of the growth of Phragmites australis: model description. *Aquatic Botany, 67*(4), 301-318. doi: http://dx.doi.org/10.1016/S0304-3770(00)00095-4

Atkinson, P. M. (2005). Sub-pixel target mapping from soft-classified, remotely sensed imagery. *Photogrammetric Engineering and Remote Sensing, 71*(7), 839-846.

Bardossy, A., & Samaniego, L. (2002). Fuzzy rule-based classification of remotely sensed imagery. *Geoscience and Remote Sensing, IEEE Transactions on, 40*(2), 362-374.

Binaghi, E., Brivio, P. A., Ghezzi, P., & Rampini, A. (1999). A fuzzy set-based accuracy assessment of soft classification. *Pattern Recognition Letters, 20*(9), 935-948. doi: http://dx.doi.org/10.1016/S0167-8655(99)00061-6

Burrough, P. A., McDonnell, R., Burrough, P. A., & McDonnell, R. (1998). *Principles of geographical information systems* (Vol. 333): Oxford university press Oxford.

Campbell, J. B. (1981). Spatial correlation-effects upon accuracy of supervised classification of land cover. *Photogrammetric Engineering and Remote Sensing, 47*(3), 355-363.

Chen, D. M., & Stow, D. (2002). The effect of training strategies on supervised classification at different spatial resolutions. *Photogrammetric Engineering and Remote Sensing, 68*(11), 1155-1161.

Chopra, R., Verma, V. K., & Sharma, P. K. (2001). Mapping, monitoring and conservation of Harike wetland ecosystem, Punjab, India, through remote sensing. *International Journal of Remote Sensing, 22*(1), 89-98. doi: 10.1080/014311601750038866

Congalton, R. G., & Green, K. (2008). *Assessing the accuracy of remotely sensed data: principles and practices*: CRC press.

Cracknell, A. P. (1998). Review article Synergy in remote sensing-what's in a pixel? *International Journal of Remote Sensing, 19*(11), 2025-2047. doi: 10.1080/014311698214848

Fisher, P. (1997). The pixel: A snare and a delusion. *International Journal of Remote Sensing, 18*(3), 679-685. doi: 10.1080/014311697219015

Foody, G. (1996). Approaches for the production and evaluation of fuzzy land cover classifications from remotely-sensed data. *International Journal of Remote Sensing, 17*(7), 1317-1340.

Foody, G. M. (2004). Sub-pixel methods in remote sensing *Remote sensing image analysis: Including the spatial domain* (pp. 37-49): Springer.

Foody, G. M., & Doan, H. T. X. (2006, July 31 2006-Aug. 4 2006). *Impacts of Class Spectral Variability on Soft Classification Prediction and Implications for Change Detection.* Paper presented at the Geoscience and Remote Sensing Symposium, 2006. IGARSS 2006. IEEE International Conference on.

Hammer, D. A., & Bastian, R. (1989). Wetlands ecosystems: natural water purifiers. *Constructed wetlands for wastewater treatment: municipal, industrial and agricultural, 5*.

Hixson, M., Scholz, D., Fuhs, N., & Akiyama, T. (1980). Evaluation of several schemes for classification of remotely sensed data. *Photogrammetric Engineering and Remote Sensing, 46*(12), 1547-1553.

Jones, K., Lanthier, Y., van der Voet, P., van Valkengoed, E., Taylor, D., & Fernández-Prieto, D. (2009). Monitoring and assessment of wetlands using Earth Observation: The GlobWetland project. *Journal of Environmental Management, 90*(7), 2154-2169. doi: http://dx.doi.org/10.1016/j.jenvman.2007.07.037

Ju, J., Kolaczyk, E. D., & Gopal, S. (2003). Gaussian mixture discriminant analysis and sub-pixel land cover characterization in remote sensing. *Remote Sensing of Environment, 84*(4), 550-560. doi: http://dx.doi.org/10.1016/S0034-4257(02)00172-4

Ludwig, D., Iannuzzi, T., & Esposito, A. (2003). Phragmites and environmental management: A question of values. *Estuaries, 26*(2), 624-630. doi: 10.1007/BF02823738

Lyon, J. G., & Greene, R. G. (1992). Use of aerial photographs to measure the historical areal extent of lake Erie coastal wetlands. *Photogrammetric Engineering and Remote Sensing, 58*(9), 1355-1360.

McMahan, J., Weber, K. T., & Sauder, J. (2003). Fuzzy classification of heterogeneous vegetation in a complex arid ecosystem. *Final report: Wildfire effects on rangeland ecosystems and livestock grazing in Idaho, 209*.

Nagendra, H., & Rocchini, D. (2008). High resolution satellite imagery for tropical biodiversity studies: the devil is in the detail. *Biodiversity and Conservation, 17*(14), 3431-3442.

Natuurmonumenten. (2011). *Wetland challenges : an innovation in succession management : Weerribben –Wieden National park*.

Pengra, B. W., Johnston, C. A., & Loveland, T. R. (2007). Mapping an invasive plant, Phragmites australis, in coastal wetlands using the EO-1 Hyperion hyperspectral sensor. *Remote Sensing of Environment, 108*(1), 74-81. doi: http://dx.doi.org/10.1016/j.rse.2006.11.002

Quintano, C., Fernandez-Manso, A., & Roberts, D. A. (2013). Multiple Endmember Spectral Mixture Analysis (MESMA) to map burn severity levels from Landsat images in Mediterranean countries. *Remote Sensing of Environment, 136*, 76-88. doi: 10.1016/j.rse.2013.04.017

Richards, J. A. (2013). *Remote sensing digital image analysis: an introduction*: Springer.

Schowengerdt, R. A. (2006). *Remote sensing: models and methods for image processing*: Academic press.

Schuyt, K., & Brander, L. (2004). The Economic value of World's wetlands. *WWF*.

Song, C. (2005). Spectral mixture analysis for subpixel vegetation fractions in the urban environment: How to incorporate endmember variability? *Remote Sensing of Environment, 95*(2), 248-263. doi: http://dx.doi.org/10.1016/j.rse.2005.01.002

Thomas, I. L., Benning, V. M., & Ching, N. P. (1987). Classification of remotely sensed images. *Geocarto International, 2*(3), 77-77. doi: 10.1080/10106048709354113

Valkama, E., Lyytinen, S., & Koricheva, J. (2008). The impact of reed management on wildlife: A meta-analytical review of European studies. *Biological Conservation, 141*(2), 364-374. doi: http://dx.doi.org/10.1016/j.biocon.2007.11.006

Verhoeven, J. T. A., Beltman, B., Bobbink, R., & Whigham, D. F. (2006). *Wetlands and Natural Resource Management* (Prof. Dr. Jos T. A. Verhoeven , Dr. Boudewijn Beltman, Dr. Roland Bobbink & D. D. F. Whigham Eds.): Springer Berlin Heidelberg.

Wikipedia. (2014). List of national parks in Netherlands. Retrieved 2014, 2014

Xie, Y., Sha, Z., & Yu, M. (2008). Remote sensing imagery in vegetation mapping: a review. *Journal of Plant Ecology, 1*(1), 9-23. doi: 10.1093/jpe/rtm005

Xie , Y. C., Sha , Z. Y., & Yu , M. (2008). Remote sensing imagery in vegetation mapping: a review. *Journal of Plant Ecology, 1*(1), 9-23. doi: 10.1093/jpe/rtm005

Zhang, J., & Foody, G. (1998). A fuzzy classification of sub-urban land cover from remotely sensed imagery. *International Journal of Remote Sensing, 19*(14), 2721-2738.

APPENDIX I

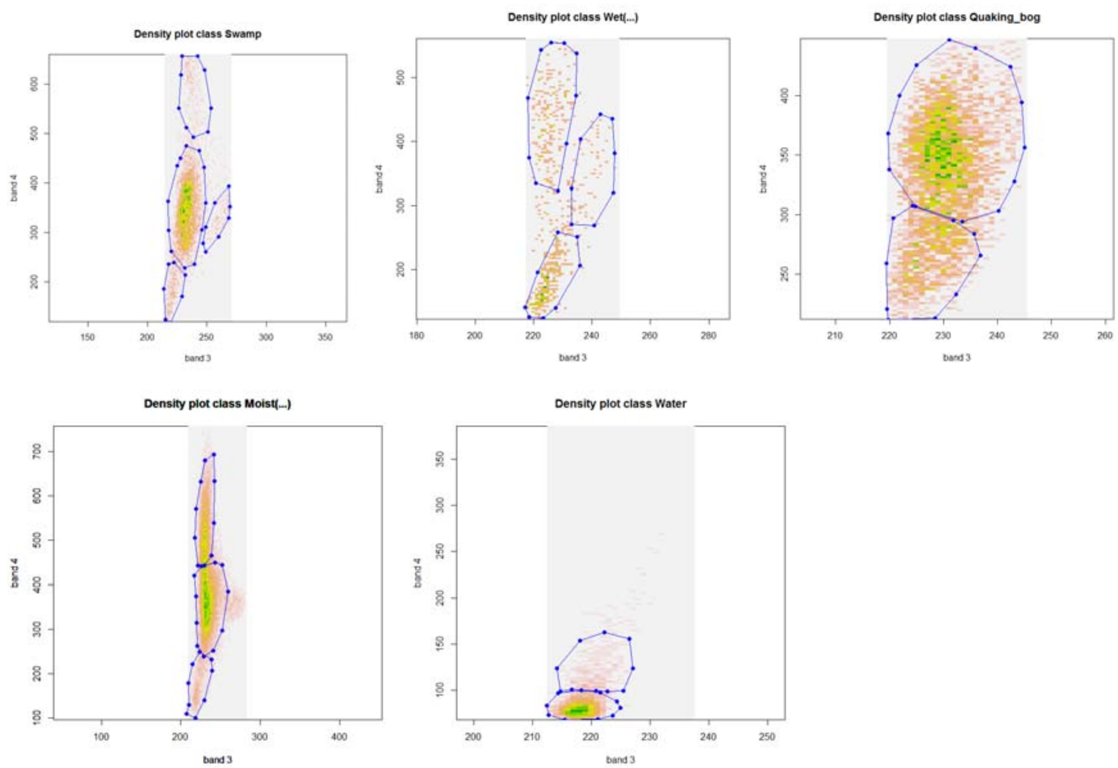

Figure I: Sub-classes identified as clusters by manual delineation. The number of clusters in a plot showed the number of subclasses within that super class. A threshold on the number of pixels displayed per class was applied to enable identification of clusters with lower density.

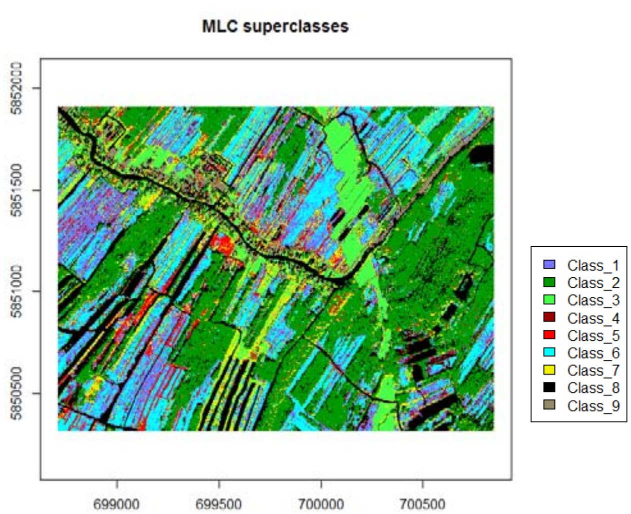

Figure_APX II: Super class Pixel based maximum likelihood classification of training site. Forest, grass and water class have highest classification accuracy.

APPENDIX II

Table I: Transformed Divergence (TD) class separability results for 21 subclasses identified. The values range with 0 to 2 for maximum and no separation respectively. Separation is shown by off diagonal values. These values show separation between subclasses on corresponding row and column.

TD	[,1]	[,2]	[,3]	[,4]	[,5]	[,6]	[,7]	[,8]	[,9]	[,10]	[,11]
[1,]	0.00	1.56	1.54	1.93	2.00	2.00	1.93	0.34	1.98	1.88	1.99
[2,]	1.56	0.00	1.90	0.94	2.00	2.00	1.98	1.20	1.99	0.48	2.00
[3,]	1.54	1.90	0.00	1.99	2.00	1.90	1.54	1.15	1.98	1.95	1.35
[4,]	1.93	0.94	1.99	0.00	2.00	2.00	2.00	1.81	2.00	0.68	2.00
[5,]	2.00	2.00	2.00	2.00	0.00	1.97	2.00	2.00	2.00	2.00	2.00
[6,]	2.00	2.00	1.90	2.00	1.97	0.00	1.53	2.00	2.00	2.00	1.11
[7,]	1.93	1.98	1.54	2.00	2.00	1.53	0.00	1.79	2.00	1.99	1.67
[8,]	0.34	1.20	1.15	1.81	2.00	2.00	1.79	0.00	1.96	1.66	1.92
[9,]	1.98	1.99	1.98	2.00	2.00	2.00	2.00	1.96	0.00	1.95	2.00
[10,]	1.88	0.48	1.95	0.68	2.00	2.00	1.99	1.66	1.95	0.00	2.00
[11,]	1.99	2.00	1.35	2.00	2.00	1.11	1.67	1.92	2.00	2.00	0.00
[12,]	1.99	1.40	2.00	1.75	2.00	2.00	2.00	1.99	2.00	1.72	2.00
[13,]	1.84	1.96	1.75	1.98	2.00	1.95	1.74	1.74	2.00	1.95	1.86
[14,]	1.32	0.54	1.43	1.42	2.00	2.00	1.90	0.88	1.74	0.84	1.99
[15,]	0.49	1.71	1.85	1.94	2.00	2.00	1.98	0.99	2.00	1.93	2.00
[16,]	0.72	1.04	1.91	1.86	2.00	2.00	1.98	0.67	1.98	1.48	2.00
[17,]	1.79	1.86	0.90	2.00	2.00	2.00	1.85	1.57	1.27	1.82	1.88
[18,]	1.93	1.98	1.27	2.00	1.98	1.43	1.45	1.71	2.00	1.97	0.97
[19,]	1.41	0.39	1.80	1.53	2.00	2.00	1.98	1.09	1.88	0.63	2.00
[20,]	1.94	0.60	1.93	1.00	2.00	2.00	1.99	1.78	1.97	0.27	2.00
[21,]	2.00	2.00	2.00	2.00	2.00	2.00	2.00	2.00	2.00	2.00	2.00

	[,12]	[,13]	[,14]	[,15]	[,16]	[,17]	[,18]	[,19]	[,20]	[,21]
[1,]	1.99	1.84	1.32	0.49	0.72	1.79	1.93	1.41	1.94	2.00
[2,]	1.40	1.96	0.54	1.71	1.04	1.86	1.98	0.39	0.60	2.00
[3,]	2.00	1.75	1.43	1.85	1.91	0.90	1.27	1.80	1.93	2.00
[4,]	1.75	1.98	1.42	1.94	1.86	2.00	2.00	1.53	1.00	2.00
[5,]	2.00	2.00	2.00	2.00	2.00	2.00	1.98	2.00	2.00	2.00
[6,]	2.00	1.95	2.00	2.00	2.00	2.00	1.43	2.00	2.00	2.00
[7,]	2.00	1.74	1.90	1.98	1.98	1.85	1.45	1.98	1.99	2.00
[8,]	1.99	1.74	0.88	0.99	0.67	1.57	1.71	1.09	1.78	2.00
[9,]	2.00	2.00	1.74	2.00	1.98	1.27	2.00	1.88	1.97	2.00
[10,]	1.72	1.95	0.84	1.93	1.48	1.82	1.97	0.63	0.27	2.00
[11,]	2.00	1.86	1.99	2.00	2.00	1.88	0.97	2.00	2.00	2.00
[12,]	0.00	2.00	1.94	2.00	1.94	2.00	2.00	1.80	1.75	2.00
[13,]	2.00	0.00	1.79	1.91	1.99	2.00	0.83	1.94	1.92	2.00
[14,]	1.94	1.79	0.00	1.72	1.31	1.03	1.85	0.65	0.91	2.00
[15,]	2.00	1.91	1.72	0.00	1.22	1.99	1.98	1.68	1.97	2.00
[16,]	1.94	1.99	1.31	1.22	0.00	1.86	2.00	0.68	1.72	2.00
[17,]	2.00	2.00	1.03	1.99	1.86	0.00	1.95	1.63	1.86	2.00
[18,]	2.00	0.83	1.85	1.98	2.00	1.95	0.00	1.96	1.92	2.00
[19,]	1.80	1.94	0.65	1.68	0.68	1.63	1.96	0.00	0.84	2.00
[20,]	1.75	1.92	0.91	1.97	1.72	1.86	1.92	0.84	0.00	2.00
[21,]	2.00	2.00	2.00	2.00	2.00	2.00	2.00	2.00	2.00	0.00

APPENDIX III

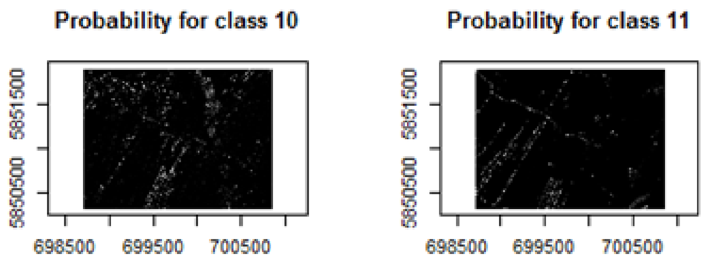

Figure III: Probability images of subclasses 10 and 11 shown as maximum and minimum probability by white and black respectively.

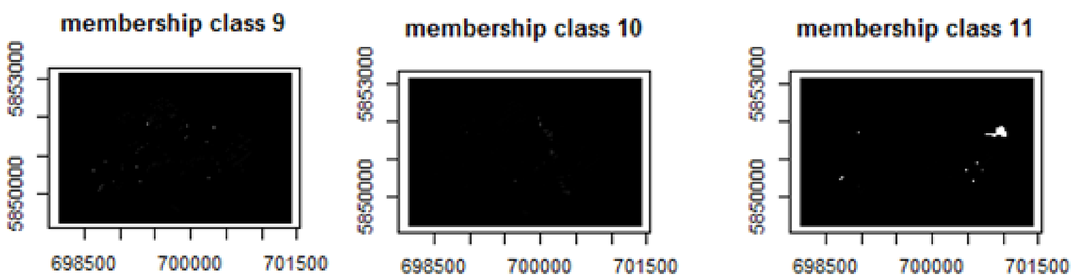

Figure IV: Membership images of subclasses 9, 10 and 11 shown as maximum and minimum by white and black respectively.

APPENDIX IV


A


B


C


D


E


F

Figure V: Photographs taken of the various land cover in The Weerribben. A shows partially mowed reed field, B shows water containing different plant types, C shows water body neighboured overshadowed by trees, D show reeds growing in trees, E show sphagnum shown on a mown field, also present on quaking bog fields and F shows the gradual transition of one land cover into other land cover.

APPENDIX V

Table II: Contingency for super class pixel based MLC. This was done using traditional MLC approach.

	Reeds	Forest	Grass	Swamp	Wet	Q.bog	Moist	Water	Total	Error of commission%	User accuracy%
Reeds	56243	2428	87	13594	103	4481	14054	1610	92600	39.26	60.74
Forest	12513	204888	911	12893	148	1430	10035	8284	251102	18.40	81.60
Grass	2416	1577	19801	1813	35	238	13403	387	39670	50.09	49.91
Swamp	8785	4565	122	4499	77	967	4178	2174	25367	82.26	17.74
Wet	7941	3174	118	3884	352	619	10963	975	28026	98.74	1.26
Q.bog	72558	4327	17	16124	178	16911	9398	772	120285	85.94	14.06
Moist	12124	8016	1615	6294	229	1072	21807	1044	52201	58.22	41.78
Water	5596	22193	311	5256	256	252	3606	56382	93852	39.92	60.08
Total	178176	251168	22982	64357	1378	25970	87444	71628	703103		
Error of ommission%	68.43	18.43	13.84	93.01	74.46	34.88	75.06	21.28			
Producer accuracy%	31.57	81.57	86.16	6.99	25.54	65.12	24.94	78.72		Overall accuracy%	54.17

Table III: Verification matrix for Sub class pixel based MLC.

	Reeds	Forest	Grass	Q.bog	Moist	Water	Total	Error of commission%	User accuracy%
Reeds	10659	2631	710	12231	6923	800	33954	68.61	31.39
Forest	2065	48350	156	745	2567	4384	58267	17.02	82.98
Grass	127	76	1199	85	12177	37	13701	91.25	8.75
Q.bog	2791	413	6	2570	1102	35	6917	62.85	37.15
Moist	1151	992	354	410	4074	431	7412	45.04	54.96
Water	35	31	0	2	13	2913	2994	2.71	97.29
Total	16828	52493	2425	16043	26856	8600	123245		
Error of	36.66	7.89	50.56	83.98	84.83	66.13			
Producer accuracy%	63.34	92.11	49.44	16.02	15.17	33.87		Overall accuracy%	56.61

Table IV: Contingency analysis; for 25 pixels threshold for crisp (top) and fuzzy (bottom) results.

	Reeds	Forest	Grass	Q.bog	Moist	Water	Total	Error of commission%	User accuracy%
Reeds	249	6	1	46	174	18	494	49.60	50.40
Forest	36	452	1	4	54	26	573	21.12	78.88
Grass	0	0	15	0	30	1	46	67.39	32.61
Q.bog	10	0	0	4	7	0	21	80.95	19.05
Moist	10	0	0	1	45	1	57	21.05	78.95
Water	5	2	0	0	3	48	58	17.24	82.76
Total	310	460	17	55	313	94	1249		
Error of ommission%	19.68	1.74	11.76	92.73	85.62	48.94			
Producer accuracy%	80.32	98.26	88.24	7.27	14.38	51.06		Overall accuracy%	65.09
Kappa coeffecient = 0.4205494									

	Reeds	Forest	Grass	Q.bog	Moist	Water	Total	Error of commission%	User accuracy%
Reeds	187.61	35.905	1.7215	36.518	143.2	18.612	423.524	55.70	44.30
Forest	42.945	407	1.2024	5.4566	55.28	26.059	537.949	24.34	75.66
Grass	4.4078	1.8342	12.246	0.1669	30.5	1.3047	50.4618	75.73	24.27
Q.bog	59.821	6.8986	0.0412	11.594	32.09	1.7389	112.18	89.66	10.34
Moist	10.545	4.3217	1.6976	1.255	47.59	2.0683	67.4784	29.47	70.53
Water	4.6737	4.0387	0.0913	0.0097	4.376	44.217	57.4071	22.98	77.02
Total	310	460	17	55	313	94	1249		
Error of ommission%	39.48	11.52	27.96	78.92	84.80	52.96			
Producer accuracy%	60.52	88.48	72.04	21.08	15.20	47.04		Overall accuracy%	56.87
Kappa coeffecient = 0.3483826									

Table V: Verification for 5 pixel threshold for crisp (top) and fuzzy (bottom) results.

	Reeds	Forest	Grass	Q.bog	Moist	Water	Total	Error of commission%	User accuracy%
Reeds	32	0	0	26	47	4	109	70.64	29.36
Forest	8	109	1	2	15	16	151	27.81	72.19
Grass	0	1	7	0	9	1	18	61.11	38.89
Q.bog	3	0	0	2	3	0	8	75.00	25.00
Moist	2	4	0	1	11	1	19	42.11	57.89
Water	0	1	0	0	0	10	11	9.09	90.91
Total	45	115	8	31	85	32	316		
Error of ommission%	28.89	5.22	12.50	93.55	87.06	68.75			
Producer accuracy%	71.11	94.78	87.50	6.45	12.94	31.25		Overall accuracy%	54.11
Kappa coeffecient = 0.3746116									

	Reeds	Forest	Grass	Q.bog	Moist	Water	Total	Error of commission%	User accuracy%
Reeds	25.837	7.5796	1.387	20.358	38.14	5.619	98.9245	73.88	26.12
Forest	8.1137	99.884	0.7578	2.6809	14.12	14.712	140.271	28.79	71.21
Grass	0.2934	1.812	4.587	0.2192	9.711	0.8451	17.4676	73.74	26.26
Q.bog	8.4628	1.0289	0.0797	6.8121	10.42	0.4778	27.2822	75.03	24.97
Moist	2.2359	3.6298	1.1885	0.929	12.59	1.269	21.8461	42.35	57.65
Water	0.0572	1.0653	2E-08	0.0003	0.008	9.0775	10.2086	11.08	88.92
Total	45	115	8	31	85	32	316		
Error of ommission%	42.58	13.14	42.66	78.03	85.18	71.63			
Producer accuracy%	57.42	86.86	57.34	21.97	14.82	28.37		Overall accuracy%	50.25
Kappa coeffecient = 0.4768523									

Table VI: Verification for 25 pixel threshold for crisp (top) and fuzzy (bottom) results.

	Reeds	Forest	Grass	Q.bog	Moist	Water	Total	Error of commission%	User accuracy%
Reeds	29	0	0	25	31	1	86	66.28	33.72
Forest	6	82	0	1	14	10	113	27.43	72.57
Grass	0	0	7	0	8	0	15	53.33	46.67
Q.bog	3	0	0	1	2	0	6	83.33	16.67
Moist	2	0	0	1	8	0	11	27.27	72.73
Water	0	0	0	0	0	8	8	0.00	100.00
Total	40	82	7	28	63	19	239		
Error of ommission%	27.50	0.00	0.00	96.43	87.30	57.89			
Producer accuracy%	72.50	100.00	100.00	3.57	12.70	42.11		Overall accuracy%	56.49
Kappa coeffecient = 0.3625									

	Reeds	Forest	Grass	Q.bog	Moist	Water	Total	Error of commission%	User accuracy%
Reeds	24.023	5.1744	1.0556	19.191	26.3	2.4947	78.2435	69.30	30.70
Forest	6.4348	75.168	0.3981	1.8665	11.92	8.8135	104.597	28.14	71.86
Grass	0.2913	0.0757	4.4207	0.2154	7.701	0.0317	12.7358	65.29	34.71
Q.bog	7.2157	0.824	0.0603	5.8093	6.892	0.1624	20.9634	72.29	27.71
Moist	1.9783	0.6364	1.0653	0.917	10.18	0.3398	15.1156	32.66	67.34
Water	0.0572	0.1212	2E-08	0.0003	0.008	7.1578	7.34468	2.54	97.46
Total	40	82	7	28	63	19	239		
Error of ommission%	39.94	8.33	36.85	79.25	83.84	62.33			
Producer accuracy%	60.06	91.67	63.15	20.75	16.16	37.67		Overall accuracy%	53.04
Kappa coeffecient = 0.3315357									

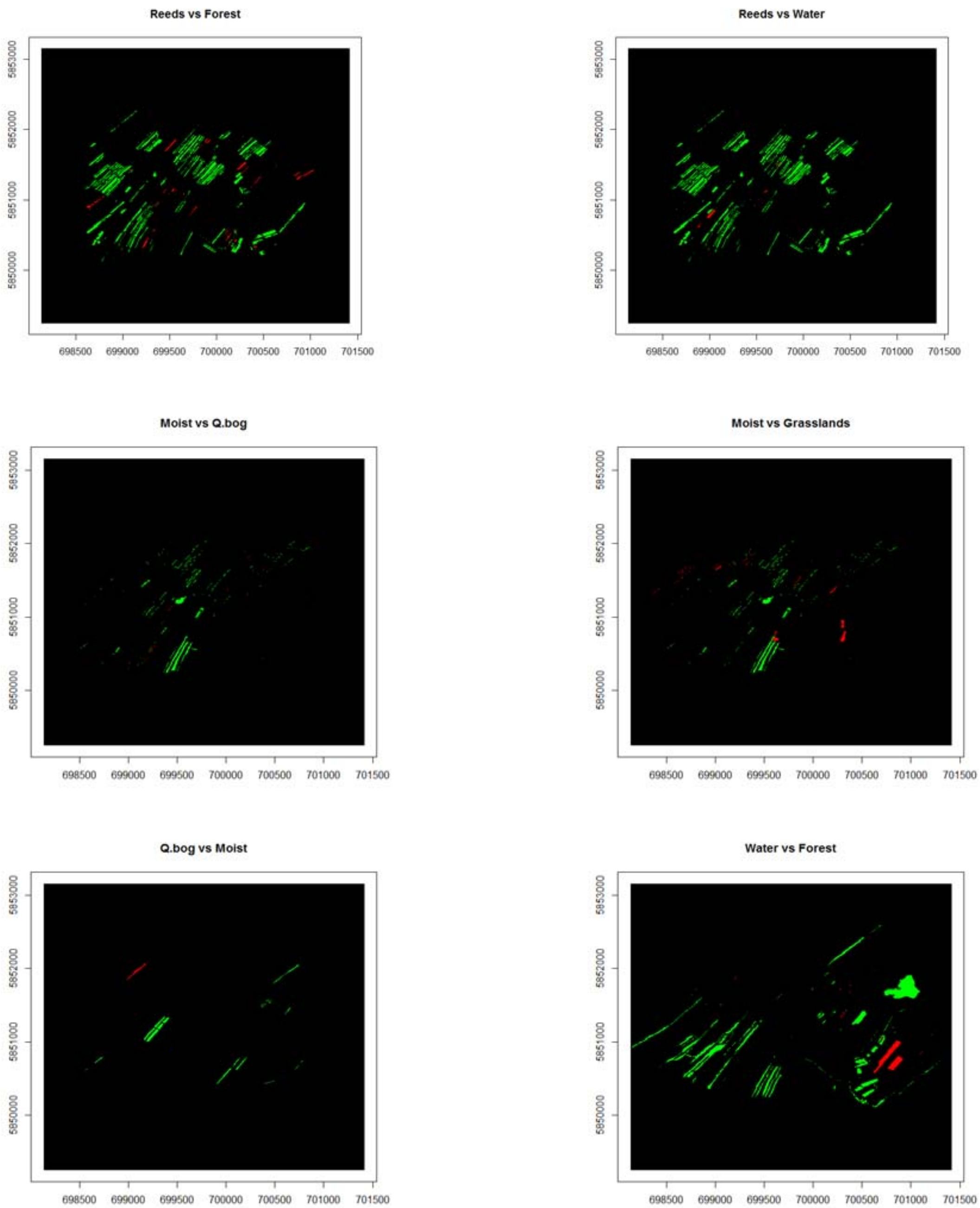

Figure VI: Positively classified parcels and misclassified parcels shown in green and red respectively. Read class a vs. class b as parcels referenced as class a (green) and misclassified as class b (red)